Victor Fernando Deorsola Sacramento

Integrity of an Offshore Structure Subjected to Waves

A Stochastic Analysis

TESE DE DOUTORADO

DEPARTMENT OF MECHANICAL ENGINEERING

Postgraduate Program in Applied Mechanics

Rio de Janeiro
January 2014

Pontifícia Universidade Católica
do Rio de Janeiro

Victor Fernando Deorsola Sacramento

Integrity of an Offshore Structure Subjected to Waves

A Stochastic Analysis

Tese de Doutorado

Thesis presented to the Postgraduate Program in Applied Mechanics of the Department of Mechanical Engineering of Centro Técnico Científico da PUC–Rio, as partial fulfillment of the requirements for the degree of Doutor em Mecânica Aplicada.

Advisor : Prof. Rubens Sampaio Filho
Co–Advisor: Prof. Thiago Gamboa Ritto

Rio de Janeiro
January 2014

Pontifícia Universidade Católica
do Rio de Janeiro

Victor Fernando Deorsola Sacramento

Integrity of an Offshore Structure Subjected to Waves

A Stochastic Analysis

Thesis presented to the Postgraduate Program in Applied Mechanics of the Department of Mechanical Engineering dof Centro Técnico Científico da PUC–Rio, as partial fulfillment of the requirements for the degree of Doutor em Mecânica Aplicada. Approved by the following commission:

Prof. Rubens Sampaio Filho
Advisor
Pontifícia Universidade Católica do Rio de Janeiro

Prof. Thiago Gamboa Ritto
Co–Advisor
Universidade Federal do Rio de Janeiro

Prof. Member 1
Pontifícia Universidade Católica do Rio de Janeiro

Prof. Member 2
Pontifícia Universidade Católica do Rio de Janeiro

Dr. Member 3
Pontifícia Universidade Católica do Rio de Janeiro

Prof. Head
Coordinator of the Centro Técnico Científico
Pontifícia Universidade Católica do Rio de Janeiro

Rio de Janeiro — January 13, 2014

Victor Fernando Deorsola Sacramento

Bibliographic data

Sacramento, Victor

Integrity of an Offshore Structure Subjected to Waves / Victor Fernando Deorsola Sacramento; advisor: Rubens Sampaio Filho; co–advisor:Thiago Gamboa Ritto . — 2014.
77 f. : il. ; 30 cm

1. Tese (Doutorado em Mecânica Aplicada) - Pontifícia Universidade Católica do Rio de Janeiro, Rio de Janeiro, 2014.

Inclui bibliografia

1. Mechanical Engineering – Teses. 2. Ondas oceânicas estocásticas. 3. Base de Karhunen Loève. 4. Modelo de ordem reduzida. 5. Dinâmica de estruturas offshore. 6. Dano em fadiga. I. Sampaio, Rubens. II. Ritto, Thiago. III. Pontifícia Universidade Católica do Rio de Janeiro. Department of Mechanical Engineering. IV. Título.

CDD: 00xx

I dedicate this work...

Acknowledgments

I'd like to say thanks to...

Abstract

Sacramento, Victor; Sampaio, Rubens; Ritto, Thiago. **Integrity of an Offshore Structure Subjected to Waves**. Rio de Janeiro, 2014. 77p. Tese de Doutorado — Department of Mechanical Engineering, Pontifícia Universidade Católica do Rio de Janeiro.

A fatigue analysis procedure was developed to evaluate the structural integrity of a drilling tower welded to an offshore platform. The tower is built from welded steel plates and it has uncertainties on the thickness of the plates and on the welds. The weld between the tower and the offshore platform is critical for fatigue and the knowledge of the probability distribution of the stress cycles on this critical point of the structure is necessary to estimate its fatigue life. The stresses on this point are given by the dynamics of the tower and the excitation of the tower is given by the dynamics of the platform (base excitation) which in turn is given by the wave loads.

Keywords

Random ocean waves. Karhunen Loève basis. Reduced-order model. Dynamics of offshore structures. Fatigue damage.

Resumo

Sacramento, Victor; Sampaio, Rubens; Ritto, Thiago. **Integridade de uma Estrutura Offshore Sujeita a Ondas**. Rio de Janeiro, 2014. 77p. Tese de Doutorado — Departamento de Mechanical Engineering, Pontifícia Universidade Católica do Rio de Janeiro.

Um procedimento para análise da fadiga...

Palavras–chave

Ondas oceânicas estocásticas. Base de Karhunen Loève. Modelo de ordem reduzida. Dinâmica de estruturas offshore. Dano em fadiga.

Contents

List of Figures

List of Tables

Nomenclature

Epigraph...

Author, *Book*.

1
Introduction

An offshore platform and all of its installed equipments should be designed for a long life span. Therefore, it is necessary to evaluate the fatigue resistance of several items during design stage. To evaluate this fatigue resistance the designer needs to obtain the dynamic response of the platform to all the external loads and thereafter to obtain the base excitation over these equipments. Given the base excitation, the dynamic response of the equipments can be calculated and the stress time history on the critical for fatigue points can be obtained and then the fatigue resistance can be determined. During all this process of determining the fatigue resistance of these equipments several assumptions have to be made by the designer and the uncertainty on them have to be considered.

The evaluation of structural integrity is a required step for the design of any offshore structure. The dynamic response of the structure due to external loads need to be investigated on early stages of the design process in order to avoid significant changes afterwards. The ocean waves are a main source of external loads and as the structure will be subjected to several different sea states during the working life of the equipment, several sea surface elevations and dynamic responses simulations should be accomplished during such investigation phase. Any reduction on the computational effort for these simulations will save working time.

Many different research areas require some source of simulation of ocean waves and structural integrity evaluation. Langley [21], investigated statistical techniques for estimating the reliability of offshore structures. He studied the reliability of an equipment modeled as a single degree of freedom system based on the available information for the intended location. Kukkanen [19] presented a procedure for the fatigue analysis of hull structures of ships. A spectral method has been applied to determine stress responses in different short-term condition and the long-term predictions for stress responses have been determined by taking into account the operational conditions of the ship. The estimative of fatigue life of the structure has been determined using Miner's fatigue accumulation hypothesis together with probabilistic models of stress

ranges and number of stress cycles. Pérez [29] was interested on testing of applications of ship motion control strategies and needed accurate and simple mathematical models to describe the exerted loads and motions of vehicles. After simulating the sea state for a given wave spectrum the results were related to the ship motion using the Response Amplitude Operators (RAO) for the specific ship. Kukkanen [20] presented a fatigue analysis procedure for offshore floating structures based on the separation of hydrodynamic load and structural responses, on the effective fatigue load concept and using response interpolation in order to simplify the fatigue analysis calculating just a few directional fatigue effective load cases. Such calculation can be accomplished in early stages of the project and can be easily updated during the development of the project. Forristall [10] needed to define the height of the deck of oil platforms and obtained statistics for the maximum crest over an area using a combination of analytical theory and numerical simulations. Forristall [11] investigated the damage caused by hurricanes Ivan, Katrina and Rita to deep water facilities and concluded that crest heights calculated using standard theories hardly could have caused such damage and calculations of the maximum crest height over the area of the deck are able to explain it. Forristall [12], studied the influence of the diffraction and radiation of the incident waves due to the large columns of a Tension Leg Platform (TLP) and estimated the maximum crests under the structure. Nielson [28] presented a method for determination of multiaxial load segments from original service histories and proposed a rainflow procedure for stress cycles counting that will be used in this work. In all these works some kind of ocean wave's simulation and structural integrity evaluation were needed. Sacramento et al [31] proposed a simplified strategy to compute the fatigue damage on a drilling tower welded to an offshore platform using the power spectral density of the wave loads and the probability distribution of the occurrence of sea states. In the present work this fatigue damage will be determined considering the uncertainty on the thickness of the plates and on the thickness of the welds as well.

This work is organized as follows. Chapter 2 presents the conceptual model for the sea surface elevation. On Chapter 3 it is shown the evaluation the dynamics of the platform. The dynamic response of the platform will be used on Chapter 4 to evaluate the dynamics of the drilling tower. The fatigue analysis is accomplished on Chapter 5. On Chapter 6 the uncertainties on the model and on the method are discussed. Results are shown on Chapter 7 and conclusions are drawn on Chapter 8. An overview of the procedure can be seen on Fig. 3.5.

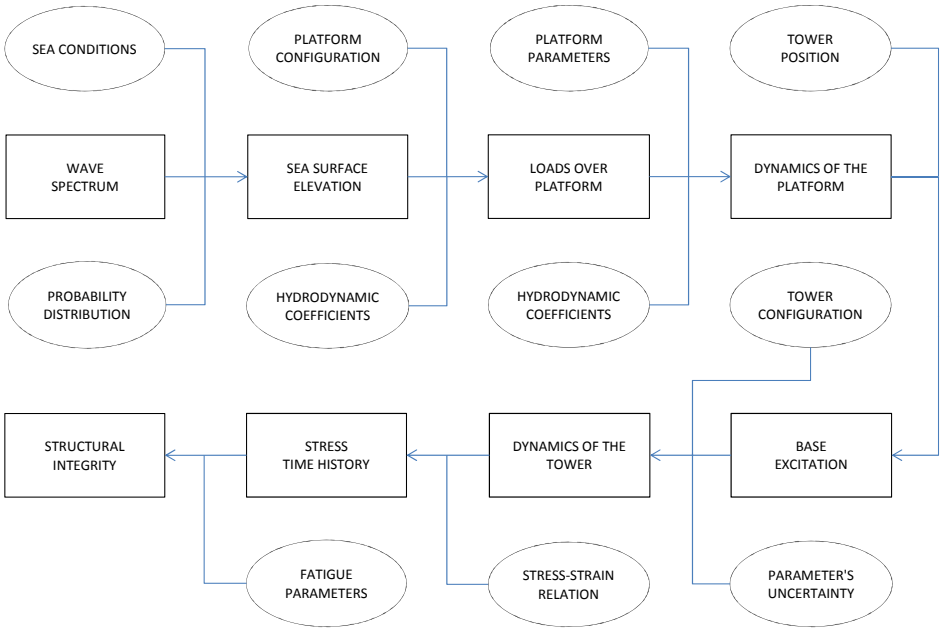

Figure 1.1: Overview of the procedure

2
Sea Surface Elevation

Ocean waves are random in terms of both time and space [29]. It is assumed that the variations of the stochastic characteristics of the sea are much slower than the variations of the sea surface itself. Therefore the elevation of the sea at a position x, y, given by $\zeta(x, y, t)$, can be considered a realization of a stationary process. The following simplifying assumptions about the underlying model are usually made

- The observed sea surface, at a certain location and for short periods of time, is considered a realization of a stationary and homogeneous, zero mean Gaussian stochastic process.
- Under a Gaussian assumption, the process, in a statistical sense, is completely characterized by the power spectral density function S

The validity of these assumptions have been investigated via analysis of time series recorded from wave riding buoys in the North Atlantic Ocean and it has been reported that

- For low and moderate sea states, significant wave height ($h_{1/3}$) lower than 4 m, the sea can be considered stationary for periods over 20 min. For more severe sea states, stationarity can be questioned even for periods of 20 min.
- For low to medium states, $h_{1/3} < 8\ m$, Gaussian models are still accurate but deviations from Gaussianity slightly increase with the increasing severity of the sea state.

In this chapter the steps to obtaining the sea surface elevation will be explained

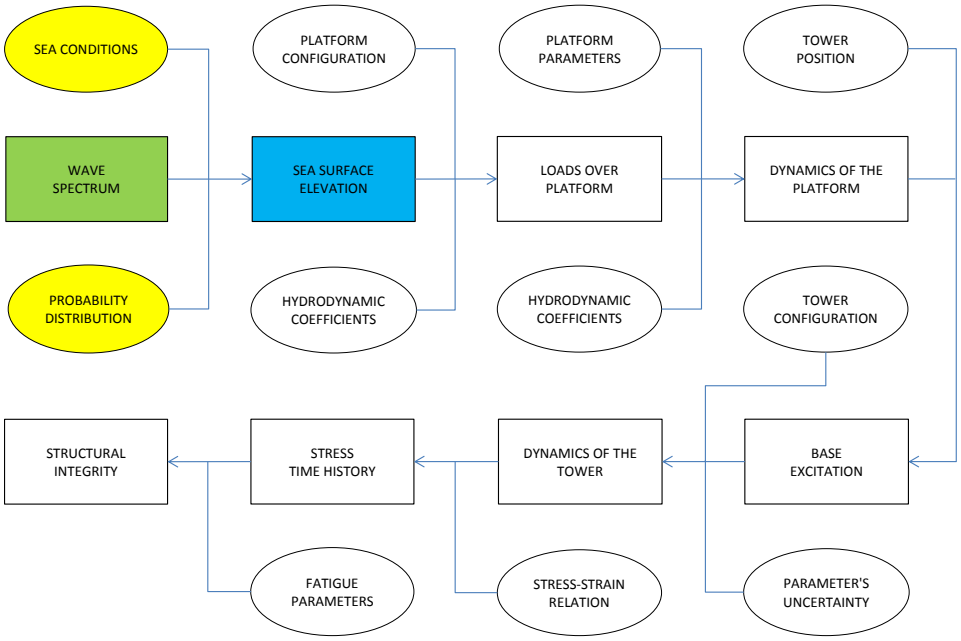

Figure 2.1: Obtaining the sea surface elevation

2.1 Regular Waves

A conceptual model to describe the sea surface elevation is given by the sum of a large number of essentially independent regular (sinusoidal) contributions with random phases. In this representation, the sea surface elevation at a location x, y with respect to a X, Y, and Z global coordinate system is given by [29]

$$\zeta(x,y,t) = \sum_{i=1}^{N} \zeta_i(x,y,t) = \sum_{i=1}^{N} \bar{\zeta}_i \cos\left(k_i x \cos\chi + k_i y \sin\chi + \omega_i t + \theta_i\right) \tag{2.1}$$

where $\zeta_i(x,y,t)$ is the contribution of the regular or harmonic traveling wave components i progressing at an angle χ with respect to the X direction and with a random phase θ_i. The parameters k_i (wave number), ω_i (wave frequency seen from a fixed position) and $\bar{\zeta}_i$ (constant wave amplitude) characterize each component. For each realization, the phase angle θ_i of each component is chosen to be a random variable with uniform distribution on the interval $[-\pi, \pi]$. This choice ensures the stationarity of $\zeta_i(x,y,t)$ [29].

For each regular wave component i, the velocity with which the wave crest moves relative to the ground, the phase velocity, is given by [29]

$$c_i = \sqrt{\frac{g\lambda_i}{2\pi}}, \quad i = 1, 2, \ldots, N \tag{2.2}$$

where g is the gravity acceleration and λ_i is the wavelength of the component i. The wave number is given by [29]

$$k_i = \frac{2\pi}{\lambda_i}, \quad i = 1, 2, \ldots, N \tag{2.3}$$

and the wave frequency is given by [29]

$$\omega_i = \sqrt{gk_i} = \frac{g}{c_i}, \quad i = 1, 2, \ldots, N \tag{2.4}$$

The Eq. 2.4 is known as the dispersion of gravity waves and establishes that the phase velocity is inversely proportional to its frequency. This means that long waves propagate faster than short ones. Considering that the observations are made at the origin of the reference frame and that the waves come from an angle of incidence $\chi = 0$ with respect to the reference frame. In this case, the Eq. 2.1 becomes [29]

$$\zeta(t) = \sum_{i=1}^{N} \zeta_i(t) = \sum_{i=1}^{N} \bar{\zeta}_i \cos\left(\omega_i t + \theta_i\right) \tag{2.5}$$

2.2 Irregular Waves

Since observed waves are not regular the wave height and frequency are not easily defined. Therefore the wave height spectral density is utilized for a statistical description of the wave elevation. The sea surface elevation can be related to its Fourier transform by [4]

$$\zeta(t) = \frac{1}{2\pi} \int_{-\infty}^{\infty} X(\omega) \exp(-i\omega t) d\omega \tag{2.6}$$

Considering the sea surface elevation an ergodic process its mean-square value can be approximated by the time average over a long period of time [4]

$$E\left\{\zeta^2(t)\right\} = \lim_{T_s \to \infty} \frac{1}{T_s} \frac{1}{2\pi} \int_{-\infty}^{\infty} |X(\omega)|^2 d\omega \tag{2.7}$$

The power spectral density (spectrum) is defined as [4]

$$S_{\zeta\zeta}(\omega) = \frac{1}{2\pi T_s} |X(\omega)|^2 \tag{2.8}$$

and the mean-square of sea surface elevation is given by [4]

$$E\left\{\zeta^2(t)\right\} = \int_{-\infty}^{\infty} S_{\zeta\zeta}(\omega) d\omega \tag{2.9}$$

The sprectrum is related to the autoorrelation function by the Wiener-Khinchine relations [4]

$$S_{\zeta\zeta}(\omega) = \frac{1}{2\pi} \int_{-\infty}^{\infty} R_{\zeta\zeta}(\tau) \exp(-i\omega\tau) d\tau \tag{2.10}$$

$$R_{\zeta\zeta}(\tau) = \int_{-\infty}^{\infty} S_{\zeta\zeta}(\omega)\exp(i\omega\tau)d\omega \tag{2.11}$$

For a zero-mean process the mean-square value equals the variance. At any particular wave frequency ω_i the variance of that component within a band Δ_ω centered at ω_i is approximated by [29]

$$\text{var}\left[\zeta_i(t)\right] = \frac{1}{2}\bar{\zeta}_i^2 \approx \int_{\omega_i-\frac{\Delta_\omega}{2}}^{\omega_i+\frac{\Delta_\omega}{2}} S_{\zeta\zeta}(\omega)d\omega \tag{2.12}$$

and the amplitudes of wave components can be approximated by [29]

$$\bar{\zeta}_i \approx \sqrt{2\int_{\omega_i-\frac{\Delta_\omega}{2}}^{\omega_i+\frac{\Delta_\omega}{2}} S_{\zeta\zeta}(\omega)d\omega} \tag{2.13}$$

For ocean applications a one-sided spectrum given in $Hertz$ (Hz) is often used. For this one-sided spectrum a superscript o is given and it can be obtained from the two-sided spectrum by the relation [4]

$$S^o_{\zeta\zeta}(\omega) = 2S_{\zeta\zeta}(\omega), \quad \omega \geq 0 \tag{2.14}$$

The two-sided spectrum given in radians can be transformed to the spectrum given in Hertz by the relation

$$S_{\zeta\zeta}(f) = 2\pi S_{\zeta\zeta}(\omega) \tag{2.15}$$

and the two-sided spectrum given in radians can be transformed to the one-sided spectrum given in Hertz by the relation

$$S^o_{\zeta\zeta}(f) = 4\pi S_{\zeta\zeta}(\omega), \quad f, \omega > 0 \tag{2.16}$$

2.3 Short-term Statistics

An irregular sea state is described by one of its statistics named significant wave height. This statistic is the average height of the highest one-third of all waves and it is found that observed wave height is consistently very close to the significant wave height [4].

When describing short-term statistics two assumptions are made, namely, stationarity and ergodicity. These assumptions are valid only for short time intervals. The wave elevation is assumed to be weakly stationary so that its autocorrelation is a function of time lag only. As a result, the mean and the variance are constant and the spectral density is invariant with time and the significant wave heigth and the significant wave period are constant when considering short term statistics. In this case the individual wave height and wave period are the random variables.

The rate at which the random process ζ crosses an elevation represented by the random variable Z with a positive slope is given by [4]

$$\nu_{z^+} = \int_0^\infty v f_{\zeta\dot{\zeta}}(z, v) dv \tag{2.17}$$

where $f_{\zeta\dot{\zeta}}$ is a joint probability density function. The expected time of the first up-crossing is given by [4]

$$E\{T\} = 1/\nu_{z^+} \tag{2.18}$$

The probability density function of the maxima is given by [4]

$$f_A(a) = \frac{\int_{-\infty}^0 -w f_{\zeta\dot{\zeta}\ddot{\zeta}}(a, 0, w) dw}{\int_{-\infty}^0 w f_{\dot{\zeta}\ddot{\zeta}}(0, w) dw} \tag{2.19}$$

where $f_{\zeta\dot{\zeta}\ddot{\zeta}}$ is a joint probability density function. If ζ is a Gaussian process the joint probability density functions are [4]

$$f_{\zeta\dot{\zeta}}(x, \dot{x}) = \frac{1}{2\pi\sigma_\zeta\sigma_{\dot{\zeta}}} \exp\left[-\frac{1}{2}\left(\frac{x}{\sigma_\zeta}\right)^2 - \frac{1}{2}\left(\frac{\dot{x}}{\sigma_{\dot{\zeta}}}\right)^2\right],$$

$$-\infty < x < \infty, -\infty < \dot{x} < \infty \tag{2.20}$$

and [4]

$$f_{\zeta\dot{\zeta}\ddot{\zeta}}(x, \dot{x}, \ddot{x}) = \frac{1}{(2\pi)^{3/2}|M|^{1/2}} \exp\left[-\frac{1}{2}\left(\{x\} - \{\mu_\zeta\}\right)^T [M]^{-1} \left(\{x\} - \{\mu_\zeta\}\right)\right] \tag{2.21}$$

where

$$[M] = \begin{bmatrix} \sigma_\zeta^2 & 0 & \sigma_{\dot{\zeta}}^2 \\ 0 & \sigma_{\dot{\zeta}}^2 & 0 \\ \sigma_{\dot{\zeta}}^2 & 0 & \sigma_{\ddot{\zeta}}^2 \end{bmatrix} \tag{2.22}$$

and

$$x - \mu_\zeta = \begin{bmatrix} x - \mu_\zeta \\ \dot{x} - \mu_{\dot{\zeta}} \\ \ddot{x} - \mu_{\ddot{\zeta}} \end{bmatrix} \tag{2.23}$$

Then, for a stationary Gaussian process, the up-crossing rate is given by [4]

$$\begin{aligned}\nu_z^+ &= \int_0^\infty f_{\zeta\dot{\zeta}}(Z,\dot{x})\dot{x}d\dot{x} \\ &= \frac{1}{2\pi\sigma_\zeta\sigma_{\dot{\zeta}}}\exp\left[-\frac{1}{2}\left(\frac{Z}{\sigma_\zeta}\right)^2\right]\int_0^\infty \exp\left[-\frac{1}{2}\left(\frac{\dot{x}}{\sigma_{\dot{\zeta}}}\right)^2\right]\dot{x}d\dot{x} \\ &= \frac{\sigma_{\dot{\zeta}}}{2\pi\sigma_\zeta}\exp\left[-\frac{1}{2}\left(\frac{Z}{\sigma_\zeta}\right)^2\right]\end{aligned} \tag{2.24}$$

and the probability density function of maxima is given by the Rice density function

$$\begin{aligned}f_A(a) &= \frac{\sqrt{1-\alpha^2}}{\sqrt{2\pi}\sigma_\zeta}\exp\left(\frac{-a^2}{2\sigma_\zeta^2\left(1-\alpha^2\right)}\right) \\ &+a\frac{\alpha}{\sigma_\zeta^2}\Phi\left(\frac{a\alpha}{\sigma_\zeta\sqrt{(\alpha^2-1)}}\right)\exp\left(\frac{-a^2}{2\sigma_\zeta^2}\right)\end{aligned} \tag{2.25}$$

where Φ is the cumulative distribution function of the standard normal random variable given by

$$\Phi(x) = \frac{1}{\sqrt{2\pi}}\int_{-\infty} x\exp\left(-z^2/2\right)dz \tag{2.26}$$

and α is the irregularity factor, equivalent to the ratio of the number of zero up-crossings to the number of peaks. This factor ranges from 0 to 1 and it is also equal to

$$\alpha = \frac{\sigma_{\dot{\zeta}}^2}{\sigma_\zeta\sigma_{\ddot{\zeta}}} \tag{2.27}$$

If ζ is a broad-band process then $\alpha = 0$ and the Rice distribution is reduced to the Gaussian probability density function given by

$$f_A(a) = \frac{1}{\sqrt{2\pi}\sigma_\zeta}\exp\left(\frac{-a^2}{2\sigma_\zeta^2}\right) \quad \text{for } -\infty < a < \infty \tag{2.28}$$

If ζ is a narrow-band process it is guaranteed that it will have a peak whenever it crosses its mean. In this case the irregularity factor is close to unity and the Rice distribution is reduced to the Rayleigh probability density function given by

$$f_A(a) = \frac{a}{\sigma_\zeta^2}\exp\left(\frac{-a^2}{2\sigma_\zeta^2}\right) \quad \text{for } 0 < a < \infty \tag{2.29}$$

That means that the amplitudes of a narrow-band stationary Gaussian process are distributed according to the Rayleigh distribution.

The maxima of ζ, A, are the amplitudes of the sea surface elevation. The wave height, $H = 2A$ is then distributed according to [4]

$$\begin{aligned} f_H(h) &= f_A H/2 \frac{dA}{dH} \\ &= \frac{h}{4\sigma_\zeta^2} \exp\left(-\frac{1}{2}\frac{h^2}{4\sigma_\zeta^2}\right) \quad \text{for } 0 < h < \infty \end{aligned} \tag{2.30}$$

For any given wave the probability that the height is less than h (the cumulative distribution) is

$$f_H(h) = 1 - \exp\left(-\frac{1}{2}\frac{h^2}{4\sigma_\zeta^2}\right) \quad \text{for } 0 < h < \infty \tag{2.31}$$

If ζ is a stationary narrow-band process so that the peaks are distributed according to the Rayleigh distribution the root-mean square of wave height is given by

$$\sqrt{E\{H^2\}} = \int_0^\infty h^2 f_H(h) dh = 2\sqrt{2}\sigma\zeta \tag{2.32}$$

In addition, it can be shown that the average wave height is given by

$$H_O \equiv E\{H\} = \sqrt{2\pi}\sigma_\zeta \tag{2.33}$$

and the significant wave heights is given by

$$H_S \equiv E\{H_{1/3}\} = 4\sigma_\zeta \tag{2.34}$$

where $E\{H_{1/3}\}$ is the expectation of the highest one-third of the waves.

2.4 Wave Spectrum

In any particular sea state, the sea surface elevation presents irregular characteristics. After the wind has blown constantly for a certain period of time the sea elevation surface becomes stationary. In this case the sea is referred to as *fully-developed*. If the irregularity of the observed waves is only in the dominant wind direction so that there are mainly uni-dimensional wave crests with carrying separation and remaining parallel to each other the sea is referred to as a *long-crested* irregular sea, [29]. For a fully-developed sea the Pierson-Moskowits (PM) spectrum for the wave amplitudes in terms of the wind velocity is given by [4]

$$S_{\zeta\zeta}^o(\omega) = \frac{8.1 \times 10^{-3} g^2}{\omega^5} \exp\left(-0.74\left(\frac{g}{V_w}\right)^4 \omega^{-4}\right) \tag{2.35}$$

where g is the gravitational constant and V_w is the wind speed at a height of 19.5m above the still water. The modal frequency, ω_m, is the one at which the spectrum is maximum. The PM spectrum can be written in terms of the modal frequency, the one at which the spectrum is the maximum. In this case it is given by

$$S^o_{\zeta\zeta}(\omega) = \frac{8.1 \times 10^{-3} g^2}{\omega^5} \exp\left(-1.25\omega_m^4 \omega^{-4}\right) \tag{2.36}$$

In some cases it may be necessary to express the spectrum in terms of the significant wave height. For a narrow band Gaussian process the significant wave height is related to the standard deviation of the sea surface elevation by Eq. 2.34, then the spectrum is given by [4]

$$S^o_{\zeta\zeta}(\omega) = \frac{8.1 \times 10^{-3} g^2}{\omega^5} \exp\left(-0.0324 \left(\frac{g}{H_S}\right)^2 \omega^{-4}\right) \tag{2.37}$$

The PM spectrum is applicable for deep water, unidirectional seas, fully developed and local-wind generated with unlimited fetch and was developed for the North Atlantic. The effect of swell is not accounted for in this spectrum anf it is found that even though it is derived for the North Atlantic the spectrum is valid for other locations [4].

2.5 Long-term Statistics

In order to predict the possible sea surface elevations that the offshore platform can be subjected to it is necessary to know the values of significant wave heights and its probability of occurrence for the location where it will be installed. For long-term statistics the significant wave height follows the Weibull distribution closely. The probability density function for a three parameter Weibull distribution is given by [4]

$$f\left(H_S\right) = \frac{m}{\beta}\left(\frac{H_s - \gamma}{\beta}\right)^{m-1} \exp\left(-\left(\frac{H_S - \gamma}{\beta}\right)^m\right) \quad \gamma < H_S \tag{2.38}$$

and the probability distribution function is given by

$$F\left(H_S\right) = 1 - \exp\left(-\left(\frac{H_S - \gamma}{\beta}\right)^m\right) \quad \gamma < H_S \tag{2.39}$$

where γ, β and m are the Weibull parameters that can be determined by least-squares methods, provided that significant wave height data over a long period of time are available. The National Data Buoy Center (NBDC) provides historical data about significant wave height collected from several stations all over the world.

Most of the commonly used probability density functions can be obtained from Weibull's equation by the proper choice of the parameters in that equation [27]. The Rayleigh probability density function for the significant wave height is given by [27]

$$f(H_S) = \frac{2H_S}{H_{rms}^2}\exp\left(-\left(\frac{H_S}{H_{rms}}\right)^2\right) \tag{2.40}$$

and by comparing the expressions in Eqs. 2.38 and 2.40 it can be noted that the Rayleigh probability density function corresponds to the parametric values of $m = 2$, $\gamma = 0$ and $\beta = H_{rms}$. The mean wave height is given by

$$H_{avg} = \int_0^\infty f(H_S) H_S dH_S \tag{2.41}$$

and considering the Weibull distribution for the significant wave height the mean value is given by

$$H_{avg} = \beta\Gamma\left(\frac{m+1}{m}\right) + \gamma \tag{2.42}$$

where Γ is the gamma function. The mean square significant wave height is given by

$$\bar{H}^2 = \int_0^\infty f(H_S) H_S^2 dH_S \tag{2.43}$$

and considering the Weibull distribution for the significant wave height the mean square and the root-mean-square are given by

$$\bar{H}^2 = H_{rms}^2 = \beta^2\Gamma\left(\frac{m+2}{m}\right) + 2\gamma\beta\Gamma\left(\frac{m+1}{m}\right) + \gamma^2 \tag{2.44}$$

Etube [9] states that for locations at North Sea the probability distribution function of significant wave height can be given by the Gumbel distribution

$$F_g(H_s) = \eta\exp\left(-\exp\left(\frac{\alpha - H_s}{\lambda}\right)\right) \tag{2.45}$$

and the probability density function is given by

$$f_g(H_s) = \frac{\eta}{\lambda}\exp\left(\frac{\alpha - H_s}{\lambda}\right)\exp\left(-\exp\left(\frac{\alpha - H_s}{\lambda}\right)\right) \tag{2.46}$$

where α, λ and η are site-dependent parameters

2.6 Reduced-order Model

The use of a sea state representation with a large number of uncorrelated sources of uncertainty in nonlinear wave body interactions leads to a computational task which may become prohibitively expensive when the statistics of extreme loads and responses are necessary [34]. Given the power spectral density of the signal an optimal set of orthogonal functions, a basis, exists

that fits the signal with the minimum number of uncorrelated sources of uncertainty [34]. This basis follows from the spectral decomposition theorems of Loève (1945) and Karhunen (1947) [2]. The Karhunen-Loève (KL) is an optimal basis to construct a reduced order model of the sea surface elevation in the sense that the projection on to the subspace generated by this basis contains the maximal amount of energy for a given number of trial functions [23]. An application for reduced-order models can be found on [30].

The use of KL basis to represent a stochastic process is based on two assumptions, the process is stationary in time and ergodic. For long periods of time the sea surface elevation is not a stationary process and as the statistical distribution of H_s is normally determined by measuring the value of H_s at three hourly interval over an extended period, [21], the process can be considered stationary only for a three hour period.

Considering the sea surface elevation at the $X = Y = 0$ coordinates the autocorrelation function of the signal is given by [34]

$$R(\tau) = E[\zeta(t)\zeta(t+\tau)] = R(-\tau) \tag{2.47}$$

Since the two-sided power spectral density of the signal $\zeta(t)$ is the Fourier transform of the autocorrelation function, Eqs. 2.10 and 2.11, the following standard relation holds [34]

$$\sigma_\zeta^2 = R(0) \tag{2.48}$$

Considering a signal over a finite time interval $(-T, T)$ the Karhunen-Loève theorem states that [34]

$$\zeta(t) = \sum_{n=0}^{\infty} \alpha_n f_n(t) \quad \text{for } -T < t < T \tag{2.49}$$

Since ζ is a stochastic process, the coefficients α_n are independent random variables such that [34]

$$E\left(\alpha_n^2\right) = \kappa_n \tag{2.50}$$

and

$$E\left(\alpha_m \alpha_n\right) = 0 \quad \text{for } m \neq n \tag{2.51}$$

The deterministic functions f_n are solutions of an eigenvalue problem cast in the form of an integral equation of the first kind with the autocorrelation function as its kernel [34]

$$\int_{-T}^{T} R(t-\tau) f_n(\tau) d\tau = \kappa_n f_n(t) \quad \text{for } n = 0, 1, \ldots \tag{2.52}$$

$$\int_{-T}^{T} f_m(\tau) f_n(\tau) d\tau = \begin{cases} 1, & m = n \\ 0, & m \neq n \end{cases} \tag{2.53}$$

$$R(t-\tau) = \sum_{n=0}^{\infty} \kappa_n f_n(t) f_n(\tau) \tag{2.54}$$

$$R(t) = \sum_{n=0}^{\infty} \kappa_n f_n(0) f_n(t) \tag{2.55}$$

$$\sigma_\zeta^2 = R(0) = \sum_{n=0}^{\infty} \kappa_n f_n(0) f_n(0)^2 \tag{2.56}$$

$$\alpha_n = \int_{-T}^{T} \zeta(t) f_n(t) dt \tag{2.57}$$

It can be observed that [34] [2]

- The independent random variables α_n are Gaussian if the signal ζ is Gaussian, which is often the case with ocean waves
- The eigenfunctions f_n are even and odd functions for positive and negative values of their argument in the range $(-T, T)$
- The rate of decay of the eigenvalues κ_n with increasing n suggests the number of the terms that are sufficient to keep in the stochastic series expansion, Eq. 2.49. If this number is small the signal is governed by a small nu,ber of independent sources of uncorrelated sources of uncertainty with statistical properties given by Eqs. 2.50 to 2.57
- The basis f_n is optimal in the sense that it allows the representation of the autocorrelation function with the minimum number of therms in the series in Eq. 2.54
- The KL representation maximizes the Shannon entropy measure which reveals the minimum number of terms that are sufficient for the representation of the variability of the signal.

In the following sections two methods of obtaining the KL basis will be explained.

2.7 Direct Method

The sea surface elevation can be decomposed in two parts [32]

$$\zeta(\mathbf{x}, t) = \mathbf{v}(\mathbf{x}, t) + E[\zeta(\mathbf{x}, t)] \tag{2.58}$$

where $\mathbf{x}$ are the X and Y coordinates of the sea surface and $\mathbf{v}$ is a stochastic process with zero mean and, as a consequence, its correlation tensor equals its autocorrelation tensor. If $\mathbf{v}$ is real then the spatial autocorrelation function of two points is defined by the tensorial product

$$R(\mathbf{x}, \mathbf{x}') = E[\mathbf{v}(\mathbf{x}, t) \otimes \mathbf{v}(\mathbf{x}', t)] \tag{2.59}$$

Considering the field

$$\mathbf{u}(x_i, y_j, t) \tag{2.60}$$

where i, j assume values from 1 to N_x, N_y respectively. For each instant of time there are N sample values, $N = 2 \times N_x \times N_y$. The number 2 multiplying the expression is due to the two fields ($x$and y). The sample can be put in order: $u_1(t), u_2(t), \ldots, u_N(t)$. The dynamic system displacement are numerically calculated in N points in M instants of time

$$[U] = [\mathbf{u}_1, \mathbf{u}_2, \ldots, \mathbf{u}_N] = \begin{bmatrix} u_1(t_1) & u_2(t_1) & \ldots & u_N(t_1) \\ . & . & . & . \\ . & . & . & . \\ . & . & . & . \\ u_1(t_M) & u_2(t_M) & \ldots & u_N(t_M) \end{bmatrix} \tag{2.61}$$

Using the stationarity and ergodicity assumption, the variation of the field with respect to the mean value is given by

$$[V] = [U] - \frac{1}{M} \begin{bmatrix} \sum_{i=1}^{M} u_1(t_i) & \sum_{i=1}^{M} u_2(t_i) & \ldots & \sum_{i=1}^{M} u_N(t_i) \\ . & . & . & . \\ . & . & . & . \\ . & . & . & . \\ \sum_{i=1}^{M} u_1(t_i) & \sum_{i=1}^{M} u_2(t_i) & \ldots & \sum_{i=1}^{M} u_N(t_i) \end{bmatrix} \tag{2.62}$$

and the spatial correlation matrix is given by

$$[R] = \frac{1}{M}[V]^T[V] \tag{2.63}$$

The matrix $[R]$ is symmetric by construction. It generates orthogonal eigenvectors, which are the Proper Orthogonal Modes also called Empirical Modes. The Proper Values are given by the eigenvalues of the matrix $[R]$. It can be noted that the dimension of matrix $[R]$ depends only on the spatial disretization. Therefore the direct method is recommended when the spatial mesh is coarse and there are many instants of time.

2.8 Snapshots Method

A snapshot is a configuration of the system at a instant of time. Using the ergodicity hypothesis a snapshot at instant m can be decomposed in two parts given by [32]

$$\mathbf{u}^{(m)} = \mathbf{v}^{(m)} + \lim_{M\to\infty} \frac{1}{M} \sum_{m=1}^{M} \mathbf{u}^{(m)} \tag{2.64}$$

After obtaining $\mathbf{v}^{(m)}$ the autocorrelation tensor is given by

$$\mathbf{R}(\mathbf{x}, \mathbf{x}') = \lim_{M\to\infty} \frac{1}{M} \sum_{m=1}^{M} \mathbf{v}^{(m)}(\mathbf{x}) \otimes \mathbf{v}^{(m)}(\mathbf{x}') \tag{2.65}$$

As in pratical applications the sum will be finite, Eq. 2.65 becomes

$$\mathbf{R}_M(\mathbf{x}, \mathbf{x}') \frac{1}{M} \sum_{m=1}^{M} \mathbf{v}^{(m)}(\mathbf{x}) \otimes \mathbf{v}^{(m)}(\mathbf{x}') \tag{2.66}$$

since M is sufficiently large. It is necessary to obtain the eigenfunctions of the tensor $\mathbf{R}_M(\mathbf{x}, \mathbf{x}')$

$$\int_D \mathbf{R}_M(\mathbf{x}, \mathbf{x})' \psi_k(\mathbf{x}') d\mathbf{x}' = \lambda_k \psi_k(\mathbf{x}) \tag{2.67}$$

$$\int_D \frac{1}{M} \sum_{m=1}^{M} \mathbf{v}^{(m)}(\mathbf{x}) \otimes \mathbf{v}^{(m)}(\mathbf{x}') \psi_k(\mathbf{x}') d\mathbf{x}' = \lambda_k \psi_k(\mathbf{x}) \tag{2.68}$$

$$\frac{1}{M} \sum_{m=1}^{M} \mathbf{v}^{(m)}(\mathbf{x}) \int_D \mathbf{v}^{(m)}(\mathbf{x}') \psi_k(\mathbf{x}') d\mathbf{x}' = \lambda_k \psi_k(\mathbf{x}) \tag{2.69}$$

Considering

$$a_{km} = \frac{1}{M} \int_D \mathbf{v}^{(m)}(\mathbf{x}') \psi_k(\mathbf{x}') d\mathbf{x}' \tag{2.70}$$

$$\sum_{m=1}^{M} a_{km} \mathbf{v}^{(m)}(\mathbf{x}) = \lambda_k \psi_k(\mathbf{x}) \tag{2.71}$$

making $A_{km} = a_{km}/\lambda_k$

$$\psi_k(\mathbf{x}) = \sum_{m=1}^{M} A_{km} \mathbf{v}^{(m)} \tag{2.72}$$

The orthogonal basis is a linear combination of the snapshots.

$$\int_D \frac{1}{M} \sum_{m=1}^{M} \mathbf{v}^{(m)}(\mathbf{x}) \otimes \mathbf{v}^{(m)}(\mathbf{x}') \sum_{m=1}^{M} A_{kn} \mathbf{v}^{(n)}(\mathbf{x}') d\mathbf{x}' = \lambda_k \sum_{m=1}^{M} A_{km} \mathbf{v}^{(m)}(\mathbf{x}) \tag{2.73}$$

$$\frac{1}{M} \sum_{m=1}^{M} \mathbf{v}^{(m)}(\mathbf{x}) \sum_{n=1}^{M} A_{kn} \int_D \mathbf{v}^{(m)}(\mathbf{x}') \mathbf{v}^{(n)}(\mathbf{x}') d\mathbf{x}' = \lambda_k \sum_{m=1}^{M} A_{km} \mathbf{v}^{(m)}(\mathbf{x}) \tag{2.74}$$

Using the internal product

$$\frac{1}{M} \sum_{m=1}^{M} \mathbf{v}^{(m)}(\mathbf{x}) \sum_{n=1}^{M} A_{kn} \left\langle \mathbf{v}^{(m)} \mathbf{v}^{(n)} \right\rangle = \lambda_k \sum_{m=1}^{M} A_{km} \mathbf{v}^{(m)}(\mathbf{x}) \tag{2.75}$$

Considering that the set of snapshots are independent, the solution of the above equation is

$$[D][A] = \lambda[A] \tag{2.76}$$

where $[A]$ is a matrix in which the columns correspond to the eigen vectors of $[D]$

$$[D]_{mn} = \frac{1}{M} \left\langle \mathbf{v}^{(m)}, \mathbf{v}^{(n)} \right\rangle \tag{2.77}$$

The construction of KL-basis results from this eigenvalue problemm. It can be noted that the dimensions of matrix [D] depends only on the number of snapshots, therefore this method is recommended when the spatial mesh is very refined and there are not many instants of time.

3
Dynamics of the Platform

An example of application of the proposed procedure will be given where the equipment to be designed is similar to the drilling tower mounted on a platform shown on Fig. 3.1.

Some simplifications on the geometry of the platform have been made and each leg of the platform will be considered to have a cylindrical shape and the connections between the legs were removed. The draft of the platform, the depth of the submerged volume of the body measured from undisturbed sea surface, has been modified in order to compensate the differences on the geometry. A sketch of the simplified platform is shown on Fig. 3.2

3.1
Equation of Motion

The motions of the platform can be split into three mutually perpendicular translations of the center of gravity G and the three rotations around G shown

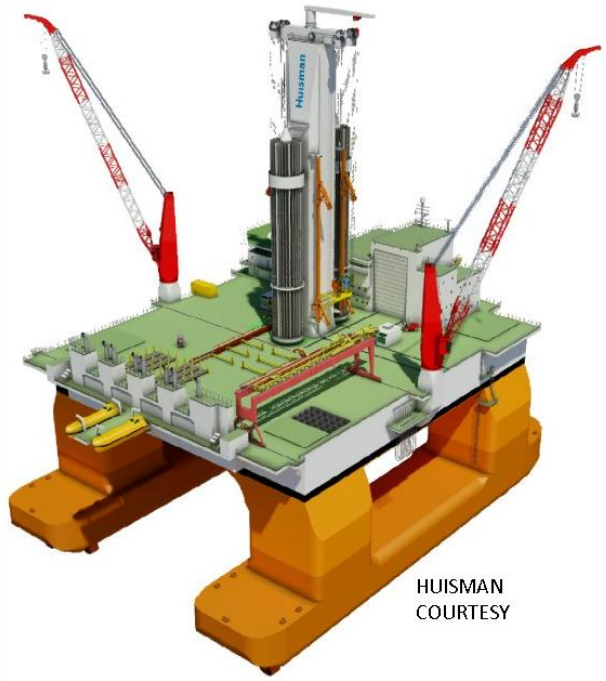

Figure 3.1: Drilling tower mounted on a platform

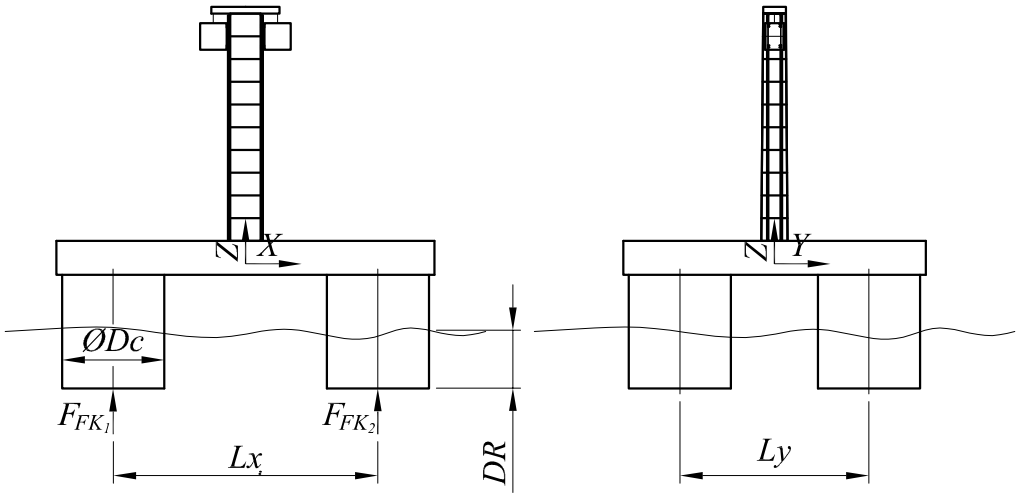

Figure 3.2: Sketch of the platform

on Fig. 3.3. When obtaining the dynamics of the platform the global coordinate system will be used.

The equations of motion for the six degrees of freedom of the platform, influenced by external loads are given by

$$\sum_{j=1}^{6} \left\{ \left(M_{ij} + A_{ij} \right) \ddot{x}_j + B_{ij} \dot{x}_j + C_{ij} x_j \right\} = F_i \quad \text{for } i = 1, \ldots, 6 \tag{3.1}$$

where $i = 1$ to 6 are the surge, sway, heave, roll, pitch and yaw motions, x_j is the displacements of harmonic oscillation in or about direction j, M_{ij} are solid mass or inertia coefficients, A_{ij} are hydrodynamic mass or inertia coefficients, B_{ij} are hydrodynamic damping coefficients and C_{ij} are restitution coefficients and F_i is the harmonic exciting wave force or moment in direction i. The surge, sway and yaw motions are considered to be restricted by the mooring system or dynamic positioning system of the platform. Therefore, in this work only the the heave, roll and pitch motions of the platform will be considered when determining the base excitation for the drilling tower.The solid mass matrix of the platform is given by

$$[M^{(p)}] = \begin{bmatrix} M_p & 0 & 0 \\ 0 & I_{xx} & -I_{xy} \\ 0 & -I_{xy} & I_{yy} \end{bmatrix} \tag{3.2}$$

where M_p is the mass of the platform, I_{xx} is the mass moment of inertia around X axis, I_{yy} is the mass moment of inertia around Y axis and I_{xy} is the mass product of inertia, when $i \neq j$. The hydrodynamic mass matrix of the platform is given by

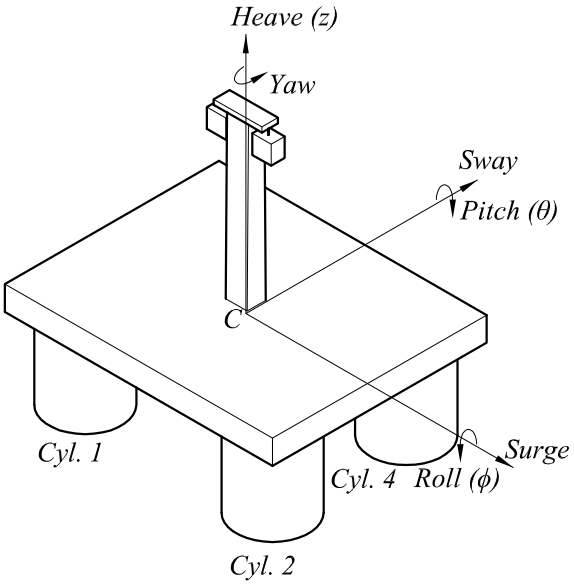

Figure 3.3: Movements of the platform

$$[A^{(p)}] = \begin{bmatrix} 4a & 0 & 0 \\ 0 & 2aL_y^2 & 0 \\ 0 & 0 & 2aL_x^2 \end{bmatrix} \tag{3.3}$$

where a is the hydrodynamic mass coefficient per cylinder of the platform, and L_x and L_y are the distances between the cylinders along X and Y direction respectively. The hydrodynamic damping matrix is given by

$$[B^{(p)}] = \begin{bmatrix} 4b & 0 & 0 \\ 0 & 2bL_y^2 & 0 \\ 0 & 0 & 2bL_x^2 \end{bmatrix} \tag{3.4}$$

where b is the hydrodynamic damping coefficient per cylinder of the platform. The restitution matrix is given by

$$[C^{(p)}] = \begin{bmatrix} 4c & 0 & 0 \\ 0 & 2cL_y^2 & 0 \\ 0 & 0 & 2cL_x^2 \end{bmatrix} \tag{3.5}$$

where c is the restitution coefficient per cylinder of the platform.

Considering that the platform motions have a linear behavior and the sea state have a known wave spectrum the resulting motions of the platform can be obtained by the superposition of the resulting motions of the platform in still water and under the action of regular waves. The following two types of loads are considered to be acting on the platform [18]

1. The hydromechanical forces and moments induced by the harmonic oscillations of the rigid body moving in the undisturbed surface of the

fluid

2. The wave exciting forces and moments produced by waves coming in on the restrained body

3.2 Hydromechanical Loads

The geometry of the platform will be simplified considering that the legs of the platform have the shape of a cylinder. The hydromechanical loads over a vertical cylinder will be discussed in the following. The dynamics of a heaving cylinder is given by [18]

$$m\ddot{z} = -P + \rho g(DR - z)A_w - b\dot{z} - a\ddot{z} \tag{3.6}$$

where m is the solid mass of the cylinder, z is the vertical displacement, P is the weight of the cylinder, ρ is the specific mass of the water, DR is the draft of cylinder at rest, A_w is the water plane area of the cylinder, b is the hydrodynamic damping coefficient and a is the hydrodynamic mass coefficient. According to Archimedes' law

$$P = \rho g DR A_w \tag{3.7}$$

and Eq. 3.6 becomes

$$(m + a)\ddot{z} + b\dot{z} + cz = 0 \tag{3.8}$$

where c is the restoring spring coefficient given by

$$c = \rho g A_w \tag{3.9}$$

The vertical oscillations of the cylinder will generate waves which propagate radially from it. Since these waves transport energy they withdraw energy from the free cylinder oscillations causing its motion die out. This so-called wave damping is proportional to the velocity of the cylinder and the coefficient b is called the wave or potential damping coefficient.

The other part of the hydromechanical force, $a\ddot{z}$, is caused by the accelerations that are given to the water particles near to the cylinder. This part of the force does not dissipate energy and manifests itself as a standing wave system near the cylinder. The coefficient a is called the hydrodynamic mass or added mass.

After experiments it could be noted that both the acceleration and the velocity terms have a sufficiently linear behavior at small amplitudes [18]. The term cz is the restoring force and the total reaction forces of the fluid on the oscillating cylinder, $a\ddot{z} + b\dot{z} + cz$, are called hydromechanical forces.

3.3 Wave Loads

In this section the steps to obtaining the loads over platform will be explained

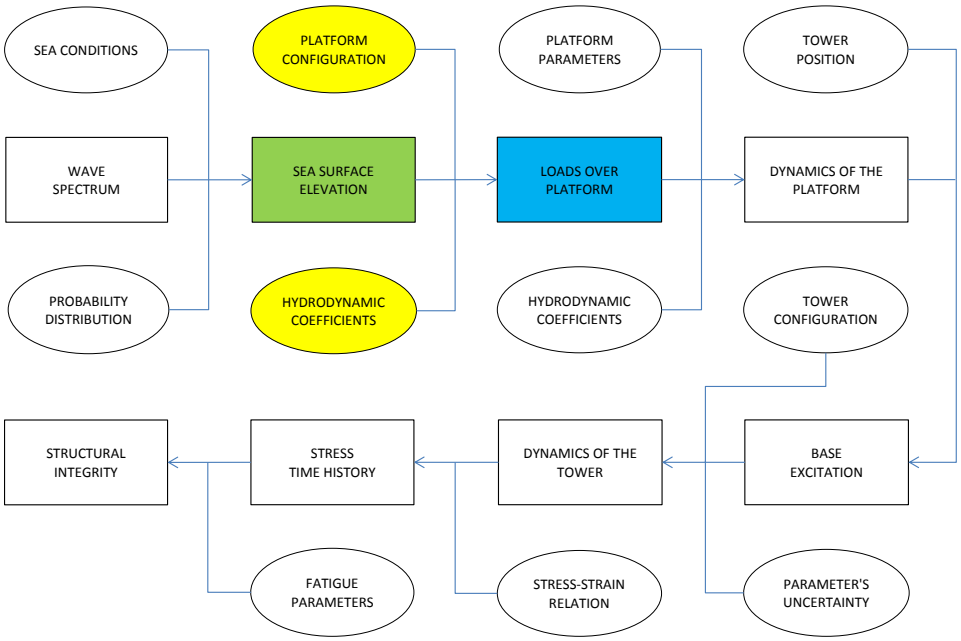

Figure 3.4: Obtaining the loads over platform

The loads due to the waves over the cylinders that represent the legs of the platform will be determined from the potential theory based on classic theory of deep water. This classic theory is based on following assumptions [18]

- The water surface slope is small, therefore terms in the equations of the waves with magnitude in the order of the steepness-squared can be ignored
- Harmonic displacements, velocities, accelerations of the water particles and also harmonic pressures will have a linear relation with the wave surface elevation, therefore the theory is considered linear

For a single regular wave traveling on x direction the wave potential is written as [18]

$$\Phi_w(x, z, t) = P(z)\sin(kx - \omega t) \tag{3.10}$$

where z is the distance below the still water level (positive upwards), k is the wave number and ω is the wave frequency. P is a function yet to be defined. This velocity potential has to fulfill four requirements:

1. Continuity, or Laplace, condition
2. Sea bed boundary condition
3. Free surface dynamic boundary condition
4. Free surface kinematic boundary condition

From the definition of the velocity potential, the velocity of the water particles in the three translational directions is given by [18]

$$\begin{aligned} u = v_x &= \frac{\partial \Phi_w}{\partial x} \\ v = v_y &= \frac{\partial \Phi_w}{\partial y} \\ w = v_z &= \frac{\partial \Phi_w}{\partial z} \end{aligned} \tag{3.11}$$

The continuity condition states that [18]

$$\frac{\partial u}{\partial x} + \frac{\partial v}{\partial y} + \frac{\partial w}{\partial z} = 0 \tag{3.12}$$

and since the fluid is homogeneous and incompressible this condition results in the Laplace Equation for potential flows [18]

$$\nabla^2 \Phi_w = \frac{\partial^2 \Phi_w}{\partial x^2} + \frac{\partial^2 \Phi_w}{\partial y^2} + \frac{\partial^2 \Phi_w}{\partial z^2} = 0 \tag{3.13}$$

Considering that water particles move in the $x - z$ plane only and substituting Eq. 3.10 into 3.13 yields a homogeneous solution of this equation [18]

$$\frac{d^2 P(z)}{dz^2} - k^2 P(z) = 0 \tag{3.14}$$

One of the solutions for P is given by

$$P(z) = C_1 e^{kz} + C_2 e^{-kz} \tag{3.15}$$

Considering the first boundary condition, the wave potential can be written now with two unknown coefficients as [18]

$$\Phi_w(x, z, t) = \left(C_1 e^{kz} + C_2 e^{-kz}\right) \sin(kx - \omega t) \tag{3.16}$$

The vertical velocity of water particles at the sea bed is zero (no-leak condition) [18]

$$\left.\frac{\partial \Phi_w}{\partial z}\right|_{z=-h} = 0 \tag{3.17}$$

where h is the sea depth at considered location. Substituting this boundary condition in Eq. 3.16 it is obtained

$$C_1 e^{-kh} = C_2 e^{kh} \tag{3.18}$$

and Eq. 3.15 can be written as

$$P(z) = \frac{C}{2}\left(e^{k(h+z)} + e^{-k(h+z)}\right) = C\cosh[k(h+z)] \tag{3.19}$$

and the wave potential with only one unknown becomes

$$\Phi_w(x,z,t) = C\cosh[k(h+z)]\sin(kx-\omega t) \tag{3.20}$$

where C is a constant to be determined. The pressure at the free surface of the fluid is equal to the atmospheric pressure. This requirement for the pressure is called the dynamic boundary condition at the free surface. The Bernoulli equation for an unsteady irrotational flow is in its general form [18]

$$\frac{\partial \Phi_w}{\partial t} + \frac{1}{2}\left(u^2+v^2+w^2\right) + \frac{p}{\rho} + gz = C^* \tag{3.21}$$

In two dimensions $v = 0$ and considering that waves have a small steepness Eq. 3.21 turns into

$$\frac{\partial \Phi_w}{\partial t} + \frac{p}{\rho} + gz = C^* \tag{3.22}$$

At the free surface this condition becomes

$$\frac{\partial \Phi_w}{\partial t} + \frac{p_0}{\rho} + g\zeta = C^* \quad \text{for } z = \zeta \tag{3.23}$$

where p_0 is the atmospheric pressure. Since $p_0/\rho - C^*$ is a constant the Eq. 3.23 can be written as

$$\frac{\partial \Phi_w}{\partial t} + g\zeta = 0 \quad \text{for } z = \zeta \tag{3.24}$$

since this equation is valid for all values of ζ it is valid for $z = 0$ as well and the wave profile becomes

$$\zeta = -\frac{1}{g}\frac{\partial \Phi_w}{\partial t} \quad \text{for } z = 0 \tag{3.25}$$

Substituting the Eq. 3.20 into 3.25 it is obtained

$$\zeta = \frac{\omega C}{g}\cosh(kh)\cos(kx-\omega t) \tag{3.26}$$

Eq. 3.26 can be written as

$$\zeta = \zeta_a \cos(kx-\omega t) \tag{3.27}$$

where

$$\zeta_a = \frac{\omega C}{g}\cosh(kh) \tag{3.28}$$

Therefore, the corresponding wave potential, as a function of the water depth, is given by

$$\Phi_w = \frac{\zeta_a g}{\omega} \frac{\cosh[k(h+z)]}{\cosh(kh)} \sin(kx - \omega t) \tag{3.29}$$

For deep water $h \to \infty$ (short waves) and the wave potential becomes

$$\Phi_w = \frac{\zeta_a g}{\omega} e^{kz} \sin(kx - \omega t) \tag{3.30}$$

The pressure on the bottom of the cylinder ($z = -DR$) can be obtained from Eq. 3.22 [18]

$$p = \rho g \zeta_a e^{-kDR} \cos(\omega t - kx) + \rho g DR \tag{3.31}$$

where DR is the draft, the distance from undisturbed sea surface to the bottom of the cylinder. Since the diameter of the cylinder is small compared to the wave length the pressure distribution on the bottom of the cylinder can be considered uniform and Eq. 3.31 turns into

$$p = \rho g \zeta_a e^{-kDR} \cos(\omega t) + \rho g DR \tag{3.32}$$

and the vertical force on the bottom of the cylinder is given by

$$F = \left[\rho g \zeta_a e^{-kDR} \cos(\omega t) + \rho g DR\right] \frac{\pi}{4} D_c^2 \tag{3.33}$$

where D_c is the diameter of the cylinder. The harmonic part of this force is the regular harmonic wave force and it can be expressed as a spring coefficient times a reduced or effective wave elevation

$$F_{FK} = c\zeta^* \tag{3.34}$$

This wave force is called the Froude-Krilov force and the spring coefficient is given by

$$c = \rho g \frac{\pi}{4} D_c^2 \tag{3.35}$$

and the reduced or effective wave elevation for deep water is given by

$$\zeta^* = e^{-kDR} \zeta_a \cos(\omega t) \tag{3.36}$$

where k is the wave number, given by

$$k_i = \frac{\omega_i^2}{g} \quad \text{for } i = 1, \ldots, N \tag{3.37}$$

The Froude-Krilov forces are obtained from an integration of the pressures on the body in the undisturbed wave. As part of the waves will be diffracted there are two additional force components, one proportional to the effective vertical acceleration and one proportional to the effective vertical velocity, therefore the total wave force on the bottom of the cylinder is given by

$$F_w = a\ddot{\zeta}^* + b\dot{\zeta}^* + c\zeta^* \tag{3.38}$$

where a is the hydrodynamic mass coefficient and b is the hydrodynamic damping coefficient. The terms $a\ddot{\zeta}^*$ and $b\dot{\zeta}^*$ are considered to be corrections on the Froude-Krilov force due to diffraction of the waves by the presence of the cylinder in the fluid. Substituting the Eq. 3.36 into 3.38 it is obtained

$$F_w = \zeta_a e{-}kDR\left(c - a\omega^2\right)\cos(\omega t) - \zeta_a e{-}kDR(b\omega)\sin(\omega t) \tag{3.39}$$

This wave force can be written independently in terms of the in-phase and out-of-phase terms

$$F_w = F_a\cos(\omega t + \varepsilon_{F\zeta}) = F_a\cos(\varepsilon_{F\zeta})\cos(\omega t) - F_a\sin(\varepsilon_{F\zeta})\sin(\omega t) \tag{3.40}$$

Equating Eqs. 3.39 and 3.40 the following equations are obtained

$$F_a\cos(\varepsilon_{F\zeta}) = \zeta_a e{-}kDR\left(c - a\omega^2\right) \tag{3.41}$$

and

$$F_a\sin(\varepsilon_{F\zeta}) = \zeta_a e{-}kDR\left(b\omega\right) \tag{3.42}$$

Adding the square of these two equations results in the wave force amplitude

$$\frac{F_a}{\zeta_a} = e^{-kDR}\sqrt{\left(c - a\omega^2\right)^2 + (b\omega)^2} \tag{3.43}$$

and the division of the in-phase and the out-of-phase term in Eq. 3.41 results in the phase shift

$$\varepsilon_{F\zeta} = \arctan\left\{\frac{b\omega}{c - a\omega^2}\right\} \quad \text{for } 0 < \varepsilon_{F\zeta}2\pi \tag{3.44}$$

Therefore, the equation of motion of a heaving cylinder under the action of hydromechanical and wave load is given by

$$(m + a)\ddot{z} + b\dot{z} + cz = a\ddot{\zeta}^* + b\dot{\zeta}^* + c\zeta^* \tag{3.45}$$

3.4 Response in Regular Waves

In this section and in the next one the steps to obtaining the dynamics of the platform will be obtained

The heave response to the regular wave excitation is given by [18]

$$z = z_a cos\left(\omega t + \varepsilon_{z\zeta}\right) \tag{3.46}$$

and substituting the Eqs. 3.46 and 3.36 into 3.45 yields

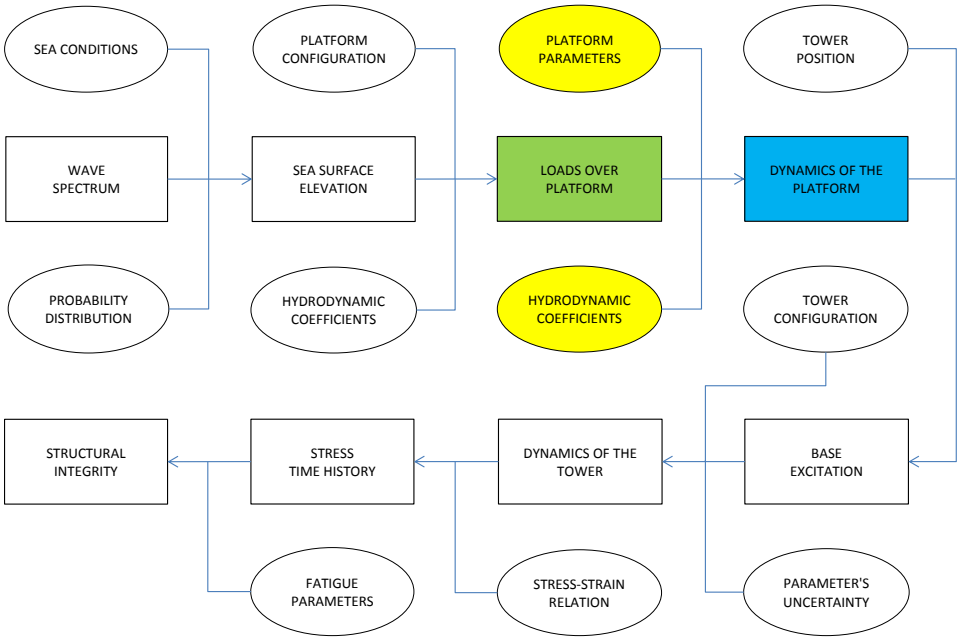

Figure 3.5: Obtaining the dynamics of the platform

$$z_a\left[c-(m+a)\omega^2\right]\cos\left(\omega t+\varepsilon_{z\zeta}\right)-z_a b\omega\sin\left(\omega t+\varepsilon_{z\zeta}\right)= \\ =\zeta_a e^{-kDR}\left(c-a\omega^2\right)\cos(\omega t)-\zeta_a e^{-kDR}b\omega\sin(\omega t) \tag{3.47}$$

By equating the two out-of-phase terms and the two in-phase terms the following two equations are obtained

$$z_a\left\{\left[c-(m+a)\omega^2\right]\cos\left(\varepsilon_{z\zeta}\right)-b\omega\sin\left(\varepsilon_{z\zeta}\right)\right\}=\zeta_a e^{-kDR}\left(c-a\omega^2\right) \tag{3.48}$$

and

$$z_a\left\{\left[c-(m+a)\omega^2\right]\sin\left(\varepsilon_{z\zeta}\right)+b\omega\cos\left(\varepsilon_{z\zeta}\right)\right\}=\zeta_a e^{-kDR}b\omega \tag{3.49}$$

Adding the squares of these two equations results in the heave amplitude characteristics

$$\frac{z_a}{\zeta_a}=e^{-kDR}\sqrt{\frac{(c-a\omega^2)^2+(b\omega)\ 2^{(}}{[c-(m+a)\omega^2)\ \ 2}\ b\omega)^2} \tag{3.50}$$

and elimination of the term $z_a/\zeta_a e^{-kDR}$ in the Eqs. 3.48 and 3.49 yields the phase shift characteristics

$$\varepsilon_{z\zeta} = \arctan\left(\frac{-mb\omega^3}{(c - a\omega^2)\left[c - (m + a)\omega^2\right) + (b\omega)^2}\right) \quad \text{for } 0 \leq \varepsilon_{z\zeta} \leq 2\pi \quad (3.51)$$

It can be noted that the requirements of linearity are fulfilled, namely, the heave amplitude is proportional to the wave amplitude and the phase shift is not dependent on the wave amplitude. The amplitude and phase characteristics are called the frequency characteristics of the vessel. The amplitude characteristics is also called the Response Amplitude Operator (RAO).

3.5 Response in Irregular Waves

The heave response spectrum of a motion can be found by using the transfer function of the motion and the wave spectrum [18]

$$S_z(\omega) = \left|\frac{z_a}{\zeta_a}(\omega)\right|^2 S_\zeta(\omega) \quad (3.52)$$

The moments of the heave response are given by

$$m_{nz} = \int_o^\infty S_z(\omega)\omega^n d\omega \quad \text{for } n = 0, 1, 2, \ldots \quad (3.53)$$

The significant heave amplitude, the mean value of the highest one-third part of the amplitudes, is given by

$$\bar{z}_{a1/3} = 2RMS = 2\sqrt{m_{0z}} \quad (3.54)$$

where RMS is the Root Mean Square value. A mean period can be found from the centroid of the spectrum

$$T_1 z = 2\pi\frac{m_{0z}}{m_{1z}} \quad (3.55)$$

The average zero-crossing period is given by

$$T_{2z} = 2\pi\sqrt{\frac{m_{0z}}{m_{1z}}} \quad (3.56)$$

Wu and Hermundstad [40] presented a nonlinear time-domain formulation for ship motions and wave loads and a nonlinear long-term statistics method. Initially they presented the theoretical long-term probability of exceedance per unit time assuming the linearity of the ship-fluid system and that the short-term response is a stationary Gaussian narrow-band process with zero mean an therefore the peak values are distributed according Rayleigh distribution. In this case the probability of exceedance per unit time is given by

$$P(y > y_1) = \int_R \int_\beta \int_H \int_T \mathrm{e}^{-y_1^2\{\}2R} np(\beta, H, T)\mathrm{d}R\mathrm{d}\beta\mathrm{d}H\mathrm{d}T \tag{3.57}$$

where y are the wave-induced loads, R is the *zeroth* spectral moment representing the mean square of each short-term response, n is the average number of maxima or minima per unit time in each short-term response, β is the wave heading, H is the wave height and T is the wave period . A completely independent calculation using Eq. 3.57 was carried out for each loading condition. Since the joint probability p is not available in advance a few simplifications were necessary and the Eq. 3.57 could be approximated by the following summation

$$P(y > y_1) = \sum_\beta \sum_{H_s} \sum_{T_1} \mathrm{e}^{-y_1^2\{\}2R} nP_1(\beta)P_2(H_s, T_1) \tag{3.58}$$

where the joint probability P_2 is presented for a given ocean area in the form of a scatter diagram. Since the nonlinear response is no longer Gaussian the distribution of peak values is not according Rayleigh distribution and Wu and Hermundstad used an alternative probability density function

$$g(y) = \frac{c}{\Gamma(r)}\mu^{cr}y^{cr-1}\mathrm{e}^{-(\mu y)^c} \quad 0 \leq y \leq \infty \tag{3.59}$$

where $\Gamma(r)$ is the gamma function and μ, c and r are parameters of the distribution that can be evaluated through certain moments of the histogram or by a weighted curve fitting and the histogram of peak values together with the average number of maxima or minima for each wave heading and sea state are obtained from the nonlinear time-domain simulation. The probability distribution function is given by

$$G(y) = \frac{\Gamma_{(uy)^c}(r)}{\Gamma(r)} \tag{3.60}$$

where $\Gamma_{()}$ is the incomplete gamma function with argument (). After some manipulation the long-term probability of exceedance for nonlinear responses is given by

$$P(y > y_1) = \sum_\beta \sum_{H_s} \sum_{T_1} \frac{(\mu y_1)^{c(r-1)}\,\mathrm{e}^{-(\mu y_1)^c}}{\Gamma(r)} nP_1(\beta)P_2(H_s, T_1) \tag{3.61}$$

Wu and Hermundstad compared the long-term obtained moments with those given by classification societies and a good agreement has been obtained and intend to use the method for accurately evaluating the extreme wave loads and other nonlinear responses in ship design.

——————————-Incluir grÃ¡ficos para pdf e PDF——————————-

4
Dynamics of the Drilling Tower

In this section the steps to obtaining the base excitation over the tower will be explained

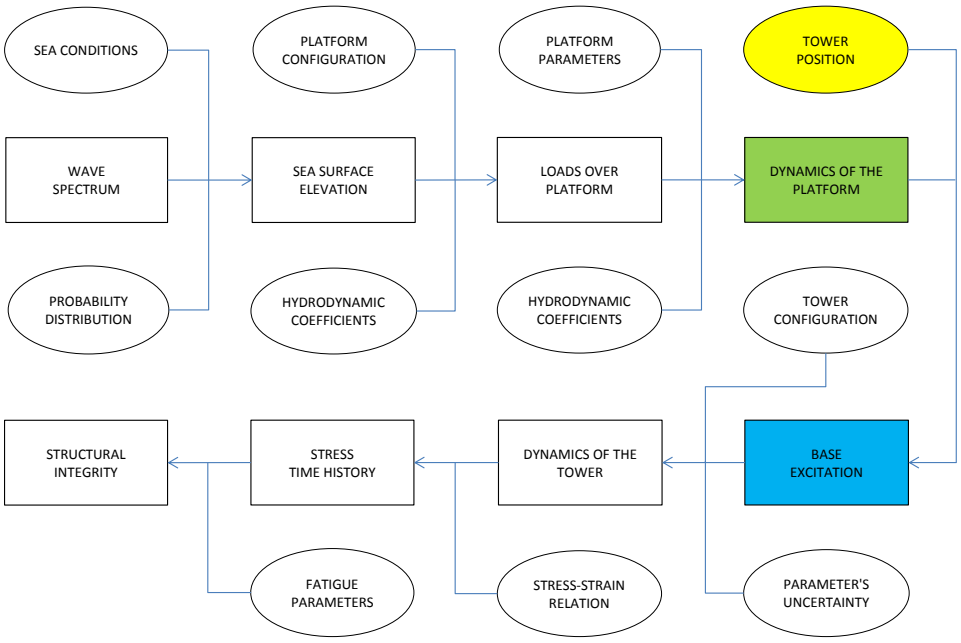

Figure 4.1: Obtaining the base excitation

The drilling tower mounted on the platform consists of a tower used to support two lifting systems. The base of the tower is welded to the platform and this weld is critical for fatigue. The base excitation on the tower is obtained by means of a coordinate transformation of the response of the platform to the x, y and z local coordinate system located at the base of the tower. The Fig. 4.2 shows the model of the tower.

4.1
Partial Differential Equation

The tower will be considered a beam clamped to the platform and free on the other end and the normal stress due to the bending about the y and z

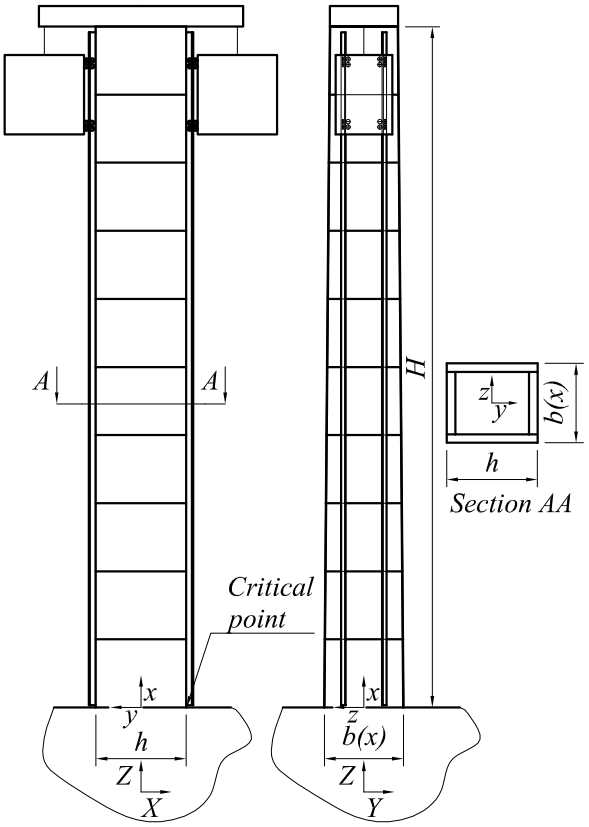

Figure 4.2: Sketch of the tower

directions will be calculated. As the mass of the tower is much smaller than the mass of the platform it will be considered that the dynamics of the tower don't affect the dynamics of the platform. The differential equation for a beam in bending around the z direction is given by

$$-\frac{\partial^2}{\partial x^2}\left[EI_z(x)\frac{\partial^2 v(x,t)}{\partial x^2}\right] + f_y(x,t) = m(x)\frac{\partial^2 v(x,t)}{\partial t^2} \quad \text{for } 0 < x < L \tag{4.1}$$

where $v(x,t)$ is the displacement on y direction of any point x and instant t, $f_y(x,t)$ is the inertia load per unit length and $I_z(x)$ is the inertia area moment about the z direction, the direction x cross the geometric center of transverse sections. The Euler-Bernoulli theory has been used. The boundary conditions for a clamped-free beam are given by

$$v(0,t) = 0 \tag{4.2}$$

$$\left.\frac{\partial v(x,t)}{\partial x}\right|_{x=0} = 0 \tag{4.3}$$

$$\left.EI_z(x)\frac{\partial^2 v(x,t)}{\partial x^2}\right|_{x=L} = 0 \tag{4.4}$$

and

$$\frac{\partial}{\partial x}\left[EI_z(x)\frac{\partial^2 v(x,t)}{\partial x^2}\right]\Bigg|_{x=L} = 0 \tag{4.5}$$

It is necessary to solve the eigenvalue problem associated to this system. As the solution for Eq.(4.1) is splittable on space and time it can be given by

$$v(x,t) = V(x)H(t) \tag{4.6}$$

where H is an harmonic function. Considering the frequency of H as ω_y, the associated eigenvalue problem can be given by the following differential equation

$$\frac{d^2}{dx^2}\left[EI_z(x)\frac{d^2V(x)}{dx^2}\right] = \omega_y^2 m(x)V(x) \quad \text{for } 0 < x < L \tag{4.7}$$

together with the following boundary conditions for a clamped-free beam

$$V(0) = 0 \tag{4.8}$$

$$\frac{dV(x)}{dx}\Bigg|_{x=0} = 0 \tag{4.9}$$

$$EI_z(x)\frac{d^2V(x)}{dx^2}\Bigg|_{x=L} = 0 \tag{4.10}$$

and

$$\frac{d}{dx}\left[EI_z(x)\frac{d^2V(x)}{dx^2}\right]\Bigg|_{x=L} = 0 \tag{4.11}$$

4.2 Approximation of the Solution

In this section the steps to obtaining the dynamics of the tower will be explained.

As the tower has a variable cross section it will be necessary to obtain an approximation of the solution to the dynamics of the structure. One of the possible ways to obtain such approximation is through the discretizing of the equations that describe the dynamics of the structure using the Finite Element Method (FEM). The equations will be discretized using one-dimensional elements with two nodes and six degrees of freedom per node as shown on Fig. 4.4.

In this work only the dynamic response of the tower on y and z direction will be investigated. An approximation of the displacement on y direction within an element is given by

$$v(x,t) \approx L_2(x)u_2(t) + L_6(x)lu_6(t) + L_8(x)u_8(t) + L_{12}(x)lu_{12}(t) \tag{4.12}$$

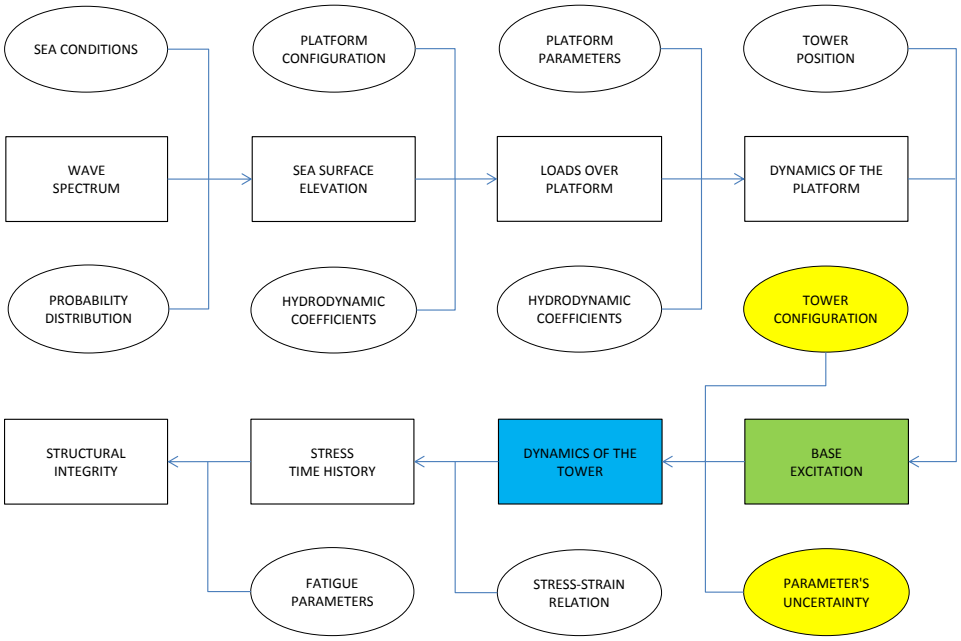

Figure 4.3: Obtaining the dynamics of the tower

where

$$\begin{aligned} L_2(x) &= (1 - 3\xi^2 + 2\xi^3) \quad L_6(x) = (-\xi - 2\xi^2 + \xi^3) \\ L_8(x) &= (3\xi^2 - 2\xi^3) \qquad L_{12}(x) = (-\xi^2 + \xi^3) \end{aligned} \tag{4.13}$$

$\xi = x/l$ and l is the length of the element. The mass and stiffness matrix obtained considering such approximations are given by

$$[M_y^{(e)}] = \frac{\rho \bar{A} l}{420} \begin{bmatrix} 156 & 22l & 54 & -13l \\ 22l & 4l^2 & 13l & -3l^2 \\ 54 & 13l & 156 & -22l \\ -13l & -3l^2 & -22l & 4l^2 \end{bmatrix} \tag{4.14}$$

and

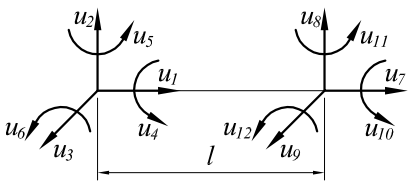

Figure 4.4: One-dimensional element

$$[K_y^{(e)}] = \frac{E\bar{I}_z}{l^3}\begin{bmatrix} 12 & 6l & -12 & 6l \\ 6l & 4l^2 & -6l & 2l^2 \\ -12 & -6l & 12 & -6l \\ 6l & 2l^2 & -6l & 4l^2 \end{bmatrix} \tag{4.15}$$

where ρ is the mass density of the material of the tower, $\bar{A}$ is the average cross section of the tower, E is the elasticity modulus and $\bar{I}_z$ is the average inertia area moment about the z direction.

As in real systems there is always some level of dissipation a damping matrix can be used. This matrix can be considered proportional to mass and stiffness matrix and is given by

$$[C_y^{(e)}] = \alpha[M_y^{(e)}] + \phi[K_y^{(e)}] \tag{4.16}$$

where α and ϕ are damping parameters. The assembly of the elements can be seen on Fig. 4.5

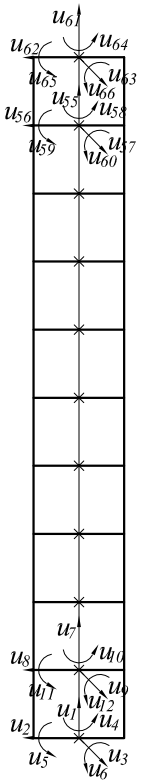

Figure 4.5: Assembly of the elements

and the approximation of the dynamics of the structure is given by

$$[M]\ddot{\mathbf{X}} + [C]\dot{\mathbf{X}} + [K]\mathbf{X} = \mathbf{F} \tag{4.17}$$

where $[M]$, $[C]$ and $[K]$ are the global matrices of the assembly of elements, $\mathbf{X}$ are the degrees of freedom of the approximation of the dynamics and $\mathbf{F}$ are the external loads over the tower.

4.3 Reduced-order Model for Dynamics

In the section 2.6 it has been proposed to use a reduced-order model to represent the sea surface elevation since the use of a full-order model to calculate the nonlinear wave body iterations is a time consuming computational task. In the same way, the use of the complete finite element model for the structure of the tower for all necessary simulations to evaluate the fatigue resistance of the equipment will make this task prohibitively expensive and an alternative reduced-order model is necessary.

Considering that the matrices $[M]$, $[C]$ and $[K]$ have dimensions $m \times m$ and a basis composed by the n elements that constitute the columns of the matrix $[\Psi]$ with dimension $m \times n$ with $n \ll m$. The dynamic response of the system represented in this basis is given by [32]

$$\mathbf{X}(t) = [\Psi]\mathbf{a}(t) \tag{4.18}$$

Substituting Eq. 4.18 into Eq. 4.17 it's obtained

$$[M][\Psi]\ddot{\mathbf{a}}(t) + [C][\Psi]\dot{\mathbf{a}}(t) + [K][\Psi]\mathbf{a}(t) = \mathbf{F}(t) \tag{4.19}$$

Matrix $[\Psi]$ is composed by orthogonal vectors, ψ_i, that generate a reduced subspace. The projection of the dynamics, Eq. 4.19, into this reduced subspace is given by

$$[M_r]\ddot{\mathbf{a}}(t) + [C_r]\dot{\mathbf{a}}(t) + [K_r]\mathbf{a}(t) = \mathbf{f}_r(t) \tag{4.20}$$

where

$$[M_r] = [\Psi]^T[M][\Psi] \tag{4.21}$$

is the reduced mass matrix,

$$[C_r] = [\Psi]^T[C][\Psi] \tag{4.22}$$

is the reduced damping matrix,

$$[K_r] = [\Psi]^T[K][\Psi] \tag{4.23}$$

is the reduced stiffness matrix and

$$[\mathbf{f}_r] = [\Psi]^T\mathbf{f} \tag{4.24}$$

is the reduced external loads vector. The system has now order $n \times n$ and it is expected that the necessary simulations to evaluate the fatigue resistance of the equipment will demand a reduced computational effort.

It is necessary to choose an efficient basis to represent the dynamics of the system. One of the options is to use the normal modes of the system. This

is the best choice when linear systems are being analyzed [32]. After solving the following eigenvalue problem

$$\left([M]\omega^2 + [K]\right)\phi = 0 \tag{4.25}$$

where ω are the natural frequencies and ϕ are the normal modes associated.

Since the base of the drilling tower is excited by the displacement of the platform and the tower is considered to be clamped to the deck of the platform, the degrees of freedom of the finite element node that represent the section of the tower close to the deck have prescribed displacements and rotations.

If the complete finite element model is being used to obtain the dynamic response of the tower, it is necessary to prescribe only the displacements and rotations of the degrees of freedom of the node at the bottom of the tower.

If in turn a reduced-order model is being used, it is necessary to associate a prescribed mode of for the entire model for each prescribed degree of freedom. In this work the finite elements used have two nodes and six degrees of freedom per node. Therefore, when constructing the reduced-order model using the normal modes from finite element model, six additional prescribed modes have to be included on the basis before accomplishing the projection of the approximation of the dynamics of the tower.

In general, the prescribed modes are given by

$$\chi = \begin{bmatrix} U_1 & U_2 & \dots & U_m \end{bmatrix}^T \tag{4.26}$$

where U_i are the prescribed values for each degree of freedom of the finite element model. The prescribed mode for the displacement of the tower on x direction is given by

$$\chi_1 = \begin{bmatrix} 1 & 0 & 0 & 0 & 0 & 0 & 1 & 0 & 0 & 0 & 0 & 0 & \dots & 1 & 0 & 0 & 0 & 0 & 0 \end{bmatrix}^T \tag{4.27}$$

The prescribed mode for the displacement of the tower on y direction is given by

$$\chi_2 = \begin{bmatrix} 0 & 1 & 0 & 0 & 0 & 0 & 0 & 1 & 0 & 0 & 0 & 0 & \dots & 0 & 1 & 0 & 0 & 0 & 0 \end{bmatrix}^T \tag{4.28}$$

The prescribed mode for the displacement of the tower on z direction is given by

$$\chi_3 = \begin{bmatrix} 0 & 0 & 1 & 0 & 0 & 0 & 0 & 0 & 1 & 0 & 0 & 0 & \dots & 0 & 0 & 1 & 0 & 0 & 0 \end{bmatrix}^T \tag{4.29}$$

The prescribed mode for the torsion of the tower around x direction is given by

$$\chi_4 = \begin{bmatrix} 0 & 0 & 0 & 1 & 0 & 0 & 0 & 0 & 0 & 1 & 0 & 0 & \dots & 0 & 0 & 0 & 1 & 0 & 0 \end{bmatrix}^T \quad (4.30)$$

The prescribed mode for the bending of the tower around y direction is given by

$$\chi_6 = \begin{bmatrix} 0 & 0 & -X_1 & 0 & 1 & 0 & 0 & 0 & -X_2 & 0 & 1 & 0 & \dots & 0 & 0 & -X_{nn} & 0 & 1 & 0 \end{bmatrix}^T \quad (4.31)$$

where X_i is the coordinate of the node i on x direction and nn is the number of nodes.

The prescribed mode for the bending of the tower around z direction is given by

$$\chi_5 = \begin{bmatrix} 0 & X_1 & 0 & 0 & 0 & 1 & 0 & X_2 & 0 & 0 & 0 & 1 & \dots & 0 & X_{nn} & 0 & 0 & 0 & 1 \end{bmatrix}^T \quad (4.32)$$

The basis for the reduced-order model is given by

$$[\Phi] = \begin{bmatrix} \chi_1 & \chi_2 & \chi_3 & \chi_4 & \chi_5 & \chi_6 & \phi_{\mathbf{1}} & \phi_{\mathbf{2}} & \dots & \phi_{\mathbf{n}} \end{bmatrix} \quad (4.33)$$

and the dynamic response is given by

$$\mathbf{X}(t) = [\Phi]\mathbf{q}(t) \quad (4.34)$$

where $\mathbf{q}$ are the modal coordinates. The approximation of the dynamics of the system projected on this basis is given by

$$[M_r]\ddot{\mathbf{q}}(t) + [C_r]\dot{\mathbf{q}}(t) + [K_r]\mathbf{q}(t) = \mathbf{f}_r(t) \quad (4.35)$$

where

$$[M_r] = [\Phi]^T[M][\Phi] \quad (4.36)$$

$$[C_r] = [\Phi]^T[C][\Phi] \quad (4.37)$$

$$[K_r] = [\Phi]^T[K][\Phi] \quad (4.38)$$

$$\mathbf{f}_r = [\Phi]^T\mathbf{f} \quad (4.39)$$

4.4 Stresses at Critical Points

In this section the steps to obtaining the stress time history will be explained.

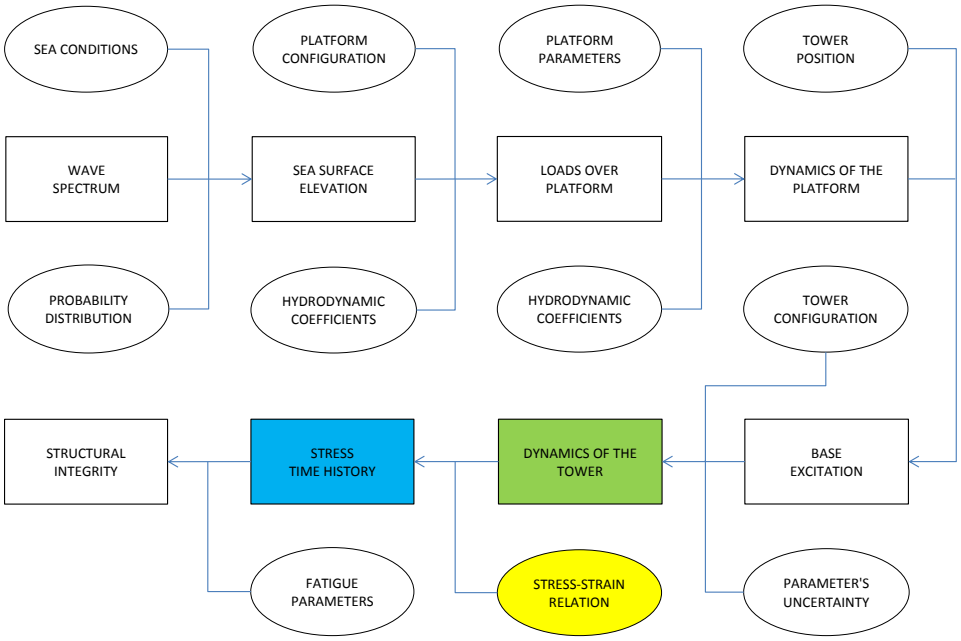

Figure 4.6: Obtaining the stress time history

The cross section of the tower is shown on Fig. 4.2. The normal stress-deformation relation for a variable cross-section beam is given by

$$\sigma(x,t) = Ey_p \frac{\partial^2 v(x,t)}{\partial x^2} \tag{4.40}$$

where y_p is the distance from required point to the neutral line of the cross section. As an approximation of the dynamics of the structure was obtained using the Finite Element Method and it is necessary to obtain an approximation to the resultant stress on required points as well. By substituting the Eq. (4.12) into Eq. (4.40) an approximation to the normal stress due to the bending about the z direction is obtained

$$\sigma(x,t) \approx Ey_p \left(L_2''(x)u_2(t) + L_6''(x)lu_6(t) + L_8''(x)u_8(t) + L_{12}''(x)lu_{12}(t)\right) \frac{\bar{I}_z}{I_z(x)} \tag{4.41}$$

where double primes indicate a double differentiation with respect to spatial variable x.

Only the steady-state part of the dynamic response of the tower should be considered when evaluating the stresses at critical points.

5
Fatigue Analysis

In this chapter the steps to calculating the structural integrity will be explained.

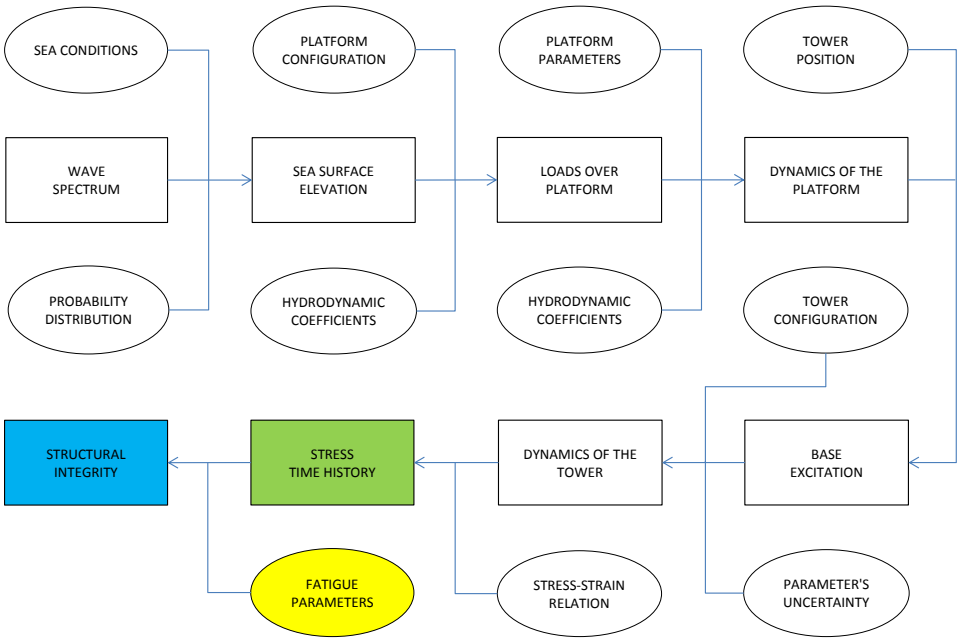

Figure 5.1: Calculating the structural integrity

In order to determine the fatigue strength of any equipment it is necessary to calculate the cumulative damage on its structure caused by cyclic loads. The expected cumulative damage for the total working life of the equipment at every point of the structure considered critical for fatigue should not exceed a critical level, [19]. In this work the fatigue life will be calculated based on the S-N fatigue approach under the assumption of linear cumulative damage.

5.1
Palmgren-Miner rule

The Palmgren-Miner rule is given by

$$D = \frac{n}{N} \tag{5.1}$$

where n is the number of stress cycles in a constant stress range S and N is the number of cycles to failure at the same constant stress range. The S-N curve for a given material and structural joint is then given by

$$NS^{m_f} = C_f \tag{5.2}$$

where m_f is the fatigue strength exponent and C_f is the fatigue strength coefficient. According to [5] the mean stresses can be neglected for fatigue assessment of welded connections and only the ranges of cyclic stress should be considered in determining the fatigue endurance. The chosen S-N curve for a given joint takes into account the local stress concentrations created by the joint itself and by the weld profile and the design stress can be considered the stress adjacent to the weld. If the weld is situated in a region of stress concentration the nominal stress should be multiplied by an appropriate stress concentration factor [5].

In this work the structural integrity of the welded connection of the base of the tower to the deck of the platform will be investigated as it is critical for fatigue and a failure in this connection would be catastrophic. Due to this criticality, [6] recommends the use of a full penetration weld and a non destructive examination after the welding process in order to check for the existence of cracks or bubbles on the weld. As the stresses were calculated using a classical beam theory a nominal stress S-N curves will be used.

5.2 Stress Range Distribution Evaluation

The use of Miner's rule together with required S-N curve to determine the fatigue strength of the structure makes necessary the knowledge of the number of stress cycles at every stress ranges for all critical points of the structure during the working life of the structure. As the fatigue strength has to be determined during the design phase of the structure it is necessary to know in advance the expected sea and loading condition, short term condition, as well their probability distribution. In this work is proposed to do a numerical simulation for each expected short term condition and construct a stress histogram to express the stress range distribution using a rainflow procedure. An approximation to the accumulated damage per each short term condition can then be given by

$$D_j = \frac{T_j}{t_j} \sum_{i=1}^{R} \frac{n_i}{\bar{N}_i} \quad \text{for } j = 1, \ldots, o \tag{5.3}$$

where o is the number of expected short term conditions, T_j is the expected working time under each short term condition, t_j is the period of the simulation, n_i is the number of stress cycles in stress block i, R is the number of stress blocks and $\bar{N}_i$ is the number of cycles to failure given by

$$\bar{N}_i = C_f \bar{S}_i^{-m_f} \quad \text{for } i = 1, \ldots, R \tag{5.4}$$

where $\bar{S}_i$ is an average stress range attributed to each stress range block. The choice of this average stress range may have a significant influence on the calculated fatigue life [5] and can be given by

$$\bar{S}_i = \lambda_i \left(S_{i-1} + S_i\right) \quad \text{for } i = 1, \ldots, R \tag{5.5}$$

where S_{i-1} and S_i are the limits for each stress block and λ_i are coefficients to be obtained from related S-N curve in order to $\bar{N}_i$ be an average number of cycles to failure at that stress block. An approximation of the probability of occurrence of the average stress range $\bar{S}_i$ is given by

$$P\left(\bar{S}_i\right) = \frac{n_i}{N_T} \quad \text{for } i = 1, \ldots, R \tag{5.6}$$

where N_T is the total number of stress cycles obtained during the simulation of the given short term condition. After substituting the Eqs. 5.4 and 5.6 into Eq. 5.3 and rearranging the accumulated damage per each short term condition can be given by

$$D_j = \frac{T_j}{t_j} \sum_{i=1}^{M} \frac{N_T P\left(\bar{S}_i\right) \bar{S}_i^m}{C} \quad \text{for } j = 1, \ldots, o \tag{5.7}$$

The summation of the product $P\left(\bar{S}_i\right) \bar{S}_i^m$ can be considered an approximation of the expected value of $\bar{S}^m$ and Eq. 5.7 can be rewritten as

$$D_j = \frac{T_j}{t_j} \frac{N_T}{C} E\left[\bar{S}^m\right] \quad \text{for } j = 1, \ldots, o \tag{5.8}$$

The total expected damage for the working life of the structure is then given by

$$D = \sum_{j=1}^{o} D_j \tag{5.9}$$

A simplified approach for fatigue analysis where the stress range distribution may be presented as a two-parameter Weibull distribution is proposed on [5]. The two-parameter Weibull probability distribution function is given by

$$F(s) = 1 - \mathrm{e}^{-(s/q)^h} \tag{5.10}$$

where s is the stress stress range, q is a scale parameter, and h is a shape parameter.

The scale parameter can be obtained from the largest stress range. In this case, it is given by [5]

$$q = \frac{s_{max}}{\left[(\ln(n_0))^{1/h}\right]} \tag{5.11}$$

where n_0 is the number of cycles and s_{max} is the largest stress range during the working life. The scale parameter, h, can be determined by least-squares methods, provided that stress range data distribution is available. In reference [5] a maximum value of $h = 1.2$ is recommended for steel structures under offshore environmental conditions.

The probability density function of the stress ranges is given by

$$f(s) = \frac{dF(s)}{ds} = h\frac{s^{h-1}}{q^h}\mathrm{e}^{-(s/q)^h} \tag{5.12}$$

The fatigue damage for finite stress range is given by Eq. 5.1 and the number of cycles to failure at a given stress range can be obtained from Eq. 5.2

$$N(s) = C_f s^{-m_f} \tag{5.13}$$

By using Eq. 5.12 and Eq. 5.13 a differential fatigue damage can be obtained as

$$dD = \frac{n_0 f(s)}{N(s)} ds \tag{5.14}$$

and an estimation of fatigue damage can be obtained as

$$\tilde{D} = \int_0^\infty dD \tag{5.15}$$

In general the S-N curves are two slope curves. Considering that the turning point is at $s = s_1$ the integration on Eq. 5.15 has to be split into

$$\tilde{D} = \tilde{D}_1 + \tilde{D}_2 \tag{5.16}$$

where

$$\tilde{D}_1 = \int_0^{s_1} \frac{n_0 f(s)}{C_{f1} s^{-m_{f1}}} ds \tag{5.17}$$

and

$$\tilde{D}_2 = \int_{s_1}^\infty \frac{n_0 f(s)}{C_{f2} s^{-m_{f2}}} ds \tag{5.18}$$

Evaluating the integral on Eq. 5.17 it is obtained

$$\tilde{D}_1 = \frac{1}{a}\left\{ n_0 \left[\left(\frac{1}{q}\right)^h\right]^{\frac{-m}{h}} \left(\frac{1}{q}\right)^{-h} q^{-h} \left[\Gamma\left(\frac{h+m}{h}, 0\right) - \Gamma\left(\frac{h+m}{h}, \left(\frac{s_1}{q}\right)^h\right)\right]\right\} \tag{5.19}$$

and evaluating the integral on Eq. 5.18 it is obtained

$$\tilde{D}_2 = \frac{1}{a}\left\{ n_0 \left[\left(\frac{1}{q}\right)^h\right]^{\frac{-m}{h}} \left(\frac{1}{q}\right)^{-h} q^{-h}\Gamma\left(\frac{h+m}{h},0\right) + \frac{1}{h(h+m)}\left\{ s_1^{h+m} \right.\right.$$

$$\left.\left.\left[\left(\frac{s_1}{q}\right)^h\right]^{-\frac{h+m}{h}} \left[-h\Gamma\left(2+\frac{m}{h},0\right) + (h+m)\Gamma\left(\frac{h+m}{h},\left(\frac{s_1}{q}\right)^h\right)\right]\right\}\right\} \tag{5.20}$$

where Γ is the gamma function given by

$$\Gamma(h,s_1) = \int_{s_1}^{\infty} s^{h-1}\mathrm{e}^{-s}ds \tag{5.21}$$

This estimation of fatigue damage may be used within an optimization strategy on intermediate calculating steps in order to reduce the computational effort.

Low, [24], presented a closed form to estimate the fatigue damage for a narrowband process. For a narrowband process the average frequency of the peaks may be approximated by the zero mean upcrossing rate which, for a Gaussian process, is given by

$$v_X^+(0) = \frac{1}{2\pi}\frac{\sigma_{\dot{X}}}{\sigma_X} \tag{5.22}$$

where X is the stochastic process, σ denotes the standard deviation a a dot the time derivative. In this case the probability density function of the peaks follows a Rayleigh distribution and is given by

$$f_R r = \frac{r}{\sigma_X^2}\mathrm{e}\left(-\frac{r^2}{2\sigma_X^2}\right) \tag{5.23}$$

The number of stress cycles in a time duration T is given by

$$n = v_X^+(0)T \tag{5.24}$$

Integrating over the stress range the expected damage can be calculated as

$$\bar{D} = v_X^+(0)T\int_0^{\infty}\frac{1}{N(s)}f_S(s)ds \tag{5.25}$$

substituting the S-N relationship it is obtained

$$\bar{D} = \frac{v_X^+(0)T}{C_f}\int_0^{\infty} s^{m_f} f_S(s)ds \tag{5.26}$$

for a narrowband process the stress range can be consiedered as

$$S = 2R \tag{5.27}$$

Substituting the Eq. 5.27 into Eq. 5.26

$$\bar{D} = \frac{2^{m_f} v_X^+(0) T}{C_f} \int_0^\infty r^{m_f} f_R(r) dr \tag{5.28}$$

Substituting the Eq. 5.23 into Eq. 5.26 and integrating, the Rayleigh approximation is obtained

$$\bar{D} = \frac{v_X^+(0) T}{C^{m_f}} \left(2\sqrt{2}\sigma_X\right)^{m_f} \Gamma\left(1 + \frac{m}{2}\right) \tag{5.29}$$

If the process can not be considered narrowbanded the Rayleigh approximation is a conservative estimate to the fatigue damage.

Fricke et al [13] compared the results obtained for the fatigue resistance of a detail of a containership according several classification societies and concluded that a variation on the predicted fatigue lives is significant, mainly due to considered loads, local stresses and chosen S-N curves. A direct calculation of loads using a spectral method was performed and the variation of the predicted life was reduced but was still significant. The results obtained by direct calculation were considered to be too conservative. It can be concluded that even using simplified approaches recommended by classification societies or direct calculation of expected fatigue lives a lot of uncertainty is presented on results.

Sutherland and Veers [36] examined the effects of using various models for the distribution of stress cycles over the structure of wind turbine components. They used a generalized Weibull fitting technique and obtained good results for matching the body of the distribution and extrapolating the tail of the distribution.

Tasdemir and Nohut [37] investigated the fatigue resistance of primary supporting members of a ship structure. They used a global finite element model for the ship and a local finite element model to obtain the stress concentration factors for the weld details. For the long term stress range distribution they used the procedure recommended by a classification society based on the Weibull distribution.

Dong et all [7] performed a long-term fatigue analysis of welded multiplanar tubular joints for a fixed jacket offshore wind turbine. They investigated the influence of the wave loads, the wind loads and the combined effect of wind and wave loads over the fatigue resistance of the welds of the structure. For the distribution of the stresses due to the wave and wind loads they used a two-parameter Weibull distribution and for the combination of wind and wave loads they used the generalized gamma function whose probability density function is given by

$$f_g(s) = \frac{|h|}{\Gamma(a)} \frac{s^{ah-1}}{q^{ah}} \mathrm{e}^{-(s/q)^h} \tag{5.30}$$

Low and Cheung [26] proposed a customized approach for assessing the fatigue resistance of mooring lines and risers. They used the JONSWAP spectrum for calculating the sea surface elevation. Since this spectrum is a function of shape parameter, the significant wave height, H_S and the spectral peak period, T_p, and they selected the value of the shape parameter, the joint probability density function of H_S and T_p is expressed as

$$f_j\left(H_S, T_p\right) = f_H\left(H_S\right) f_{TH}\left(T_p | H_S\right) \tag{5.31}$$

Considering $d\left(H_S, T_p\right)$ as the damage function for a given H_S and T_p pair, Low and Cheung proposed to calculate the expected long-term damage accumulated over a period T as

$$E[D] = T \int_0^\infty T \int_0^\infty d\left(H_s, T_p\right) f_j\left(H_s, T_p\right)(d) H_S(d) T_p \tag{5.32}$$

and they proposed to use a multi-peaked third-order asymptotic approximation for the integrand in order to evaluate this probability integral.

In most of the cases the stresses on structural components are a combination of two or more stresses due to different loads. Leira [22] investigated the fatigue damage of welds subjected to multiple stress components. Despite of the stress cycles of each individual component being distributed according Weibull distribution even a linear combination of two or more Weibull components wil in general not be Weibull distributed [22]. Leira proposes that for the linear combination of two stress components with Weibull cycle distributions the fatigue damage which is accumulated during a time period T for a one-slope S-N curve expressed according Eq. 5.2 can be expressed as

$$E[D(T)] = \frac{N(T)}{C_f} \int_0^\infty T \int_0^\infty \left[\sqrt{s_1^2 + c s_2^2}\right]^m \times f_{s_1 s_2}(s_1, s_2)(d) s_1(d) s_2 \tag{5.33}$$

where $N(T)$ is the number of stress cycles that occur during the period T, s_1 and s_2 are the stress components, c is a constant to obtain the combined stress and $f_{s_1 s_2}$ is the joint probability density function. Leira investigated the effect of correlation between the two stress components on fatigue damage.

Ang et al [1] developed a technical procedure for a reliability-based approach to fatigue analysis and fatigue-resistant design. They considered that the stress cycles can be distributed according a Beta distribution whose probability density function is given by

$$f_b(s) = \frac{s^{q-1}}{\beta(q, r)} \frac{\left(s_u - s\right)^{r-1}}{s_u^{q+r-1}} \quad 0 \leq s \leq s_u \tag{5.34}$$

where s are the stress ranges, s_u is a upper limit for the stress ranges and

$$\beta(q,r) = \frac{\Gamma(q)\Gamma(r)}{\Gamma(q+r)} \tag{5.35}$$

where Γ is the gamma function and q and r are parameters of distribution given by

$$q = \frac{\mu}{s_u}\left[\Omega^{-2}\left(\frac{s_u}{\mu}-1\right)-1\right] \tag{5.36}$$

and

$$r = \left(\frac{s_u}{\mu}-1\right)q \tag{5.37}$$

where μ is the mean and Ω is the covariance of the applied stress range.

Wang [39] calculated the fatigue life of a ship structural detail using a spectral approach. Assuming that the wave-induced bending stress variation in a ship structural element in a specific sea state is a narrow band gaussian random process and consequently the peak values of the stress has a Rayleigh probability density function Wang presented the following formula to calculate the fatigue damage in a specific sea state

$$D_i = \frac{T}{C_f}\left(2\sqrt{(2)}\right)^{m_f}\Gamma\left(\frac{m_f}{2}+1\right)f_{0i}p_i\left(\sigma_i\right)^{m_f} \tag{5.38}$$

where T is design life of a ship in seconds, C_f is the fatigue strength coefficient, m_f is the fatigue strength exponent, Γ is the gamma function, f_{0i} is zero-up crossing frequency of the stress response in Hz, p_i is the probability of occurrence of the sea state i and σ_i is the standard deviation of the stress process in the specific sea state.

Since for a wide band random process the Rayleigh distribution for the stress peak values will result in a conservative estimation of the fatigue damage a cycle counting correction factor in damage calculation should be introduced in order to reduce the conservatism due to the narrow band assumption. In this case the formula for fatigue damage, Eq. 5.38, has to be written as

$$D_i = \frac{T}{C_f}\left(2\sqrt{(2)}\right)^{m_f}\Gamma\left(\frac{m_f}{2}+1\right)\lambda\left(m_f,\epsilon_i\right)f_{0i}p_i\left(\sigma_i\right)^{m_f} \tag{5.39}$$

where λ is the damage correction factor. This factor is a function of the fatigue strength exponent and of ϵ_i that can be either a bandwidth parameter or a regularity factor depending on the chosen formula for calculating the cycle counting correction factor. Wang [39] presented three different formulas for calculating this factor. Using one of these formulas, Wang obtained a fatigue life of 25.16 years for a structural ship detail. For comparison, Wang also calculated the fatigue life according the recommendation of a classification society that assumes that the long-term distribution of the stresses follows a

Weibull distribution. In this case the calculated fatigue life was found to be 18.765 years.

6
Model's Uncertainties

The inherent uncertainties on the parameters or operators of any mechanical system must be considered during the evaluation of its fatigue resistance. Since the probability density function for the random variables that represent such parameters or operators are not always available in advance for the designer it is necessary a strategy to obtain the necessary probability density functions.

6.1
Maximum Entropy Principle

If there is not enough data available for the random variables the Principle of Maximum Entropy can be used to obtain an approximation of the required probability density function [35], [15] and [16]. This principle states that:

"Among all the probability distributions consistent with the prescribed conditions the one that maximizes the uncertainty (entropy) should be chosen"

Being n the number of the welds of the tower, W a random vector with n components and pW the probability density function of W, the entropy related to pW is given by

$$S\left(pW\right) = -\int_{-\infty}^{+\infty}\int_{-\infty}^{+\infty}...\int_{-\infty}^{+\infty} pW(w)\ln\left(pW(w)\right)dw\,. \tag{6.1}$$

The only available information about the random variables is the fabrication tolerance, $W_{min} \preceq W \preceq W_{max}$. By using the Principle of Maximum Entropy the obtained probability density function is

$$pW(w) = \mathbb{1}_{[W_{min},W_{max}]}(w)\prod_{i=1}^{n}\frac{1}{W_{maxi}-W_{mini}} \tag{6.2}$$

therefore, the random variables are independent with Uniform pdf. The same distribution applies to the thickness of the plates.

6.2
Uncertainties in Fatigue Life Prediction

According [5] large uncertainties are associated with fatigue life prediction. One of the sources of uncertainty are the S-N curves. Such curves are determined

by mean of experiments on specimen and the two slope exponential curves obtained by curve fitting from measured points. Further, the design curves recommended on standards are the mean curve minus two standard deviations.

Batous and Soize [3] proposed a methodology for construction and identification of a probabilistic model of random fields in presence of modeling errors in high stochastic dimension and presented in context of computational structural dynamics. They presented two ways to construct the prior stochastic model of a random field $\mathbb{H}$.

The first way is using an algebraic stochastic representation of the random field $\mathbf{H}$

$$\mathbf{H}((x)) = f_r(\mathbf{G}(\mathbf{x})) \quad \text{for } \mathbf{x} \in \Omega \tag{6.3}$$

where $\mathbf{x}$ is a vector representing any point in the open bounded domain Ω of $\mathbb{R}^3$, f_r is a given nonlinear deterministic mapping and where $\{\mathbf{G}(\mathbf{x}, \mathbf{x} \in \Omega\}$ is agiven random field for which the probability law (system of marginal probability distributions) is completely defined and for which a generator of independent realizations is available.

For the second way it is necessary that the mean function and the covariance function of random field $\mathbf{H}$ are known functions, what is the case when an algebraic stochastic representation of $\mathbf{H}$ has been constructed or if experimental data are available for estimating these two functions with a sufficient accuracy. Then under certain hypotheses a statistical reduction can be constructed using the Karhunen-Loève expansion. The first way has been used in this work for the constructing the stochastic model for the thickness of the welds and for the thickness of the plates of the drilling tower.

Veldkamp on [38] presents the uncertainties on the results of fatigue strength obtained by experiments with identical specimens under constant and variable amplitude loading. He concluded that the fatigue life under variable amplitude loading is shorter than the fatigue life under constant amplitude loading. Therefore, when the designer chooses the S-N curve to be used for the fatigue resistance evaluation of a structural component it is necessary to be aware of whether the curve was obtained using constant or variable amplitude loading. If the available curves were obtained under constant amplitude loading a reduction factor for the values of the curve have to be used. Veldkamp concluded on the same reference that the uncertainty of the fatigue parameters dominate the overall uncertainty of the fatigue resistance of the studied equipment.

Since the design of offshore equipments has to attend to the required standards, the use of Design Fatigue Factors when determining critical param-

eters for the structure has a big influence its fatigue life. Such design factors are intended to overcome the uncertainty on loading, on S-N data and on the Palmgren-Miner damage accumulation rule and to avoid the need of a probabilistic analysis of the problem.

When the weld details require the use of hot spot stress factors, the derivation of these factor is a source of uncertainty as well. The critical details that present reduced fatigue life have to be inspected in-service to check for existence of fatigue cracks.

Others sources of uncertainties are the choice of parameters for the simulation of sea surface elevation, the model for the interaction between the platform and the sea waves, the choice of hydrodynamics coefficients for evaluation of the dynamics of the platform and the finite element model to be used to obtain the stresses on required critical points.

Sarkar et al [33] proposed an approach based on Wiener chaos expansions to estimate the fatigue damage in structural systems with parameter uncertainties. They used the Hermite polynomial expansion to describe the dependence of the damage rate on some uncertain parameters

$$d(z) = \sum_{j=0}^{\infty} c_j H_j(z) \approx \sum_{j=0}^{n} c_j H_j(z) = d_n(z) \tag{6.4}$$

where d is the damage rate, z is a random variable, H_j are Hermite polynomials and

$$\begin{aligned} c_j = E\left[d(z)H_j(z)\right] &= \tfrac{1}{\sqrt{2\pi}} \int_{-\infty}^{+\infty} d(z)H_j(z)(e)^{-z^2/2}\mathrm{d}z \\ &\approx \tfrac{1}{\sqrt{2\pi}} \sum_{i=1}^{n} h_i d(z_i)H_j(z_i)\mathrm{e}^{-z_i^2/2} \end{aligned} \tag{6.5}$$

Sarkar et al used this expansion to quantify how the uncertainty of one of the parameters of the Morison's equation used to model the force acting on the pile of an offshore structure. They calculated the damage rate using a three term truncated Hermite expansion and compared with the results obtained using rainflow technique. A good agreement between the two estimates was obtained, even in the tails of the distribution of z.

Low [25] presented a method for analyzing the variance of the damage for any narrow-band Gaussian process. The covariance of the damage is given by

$$c_D^2 = \frac{N + 2\chi}{N^2} \left(\frac{\Gamma(1 + m_f}{\Gamma(1 + m_f/2) - 1} \right) \tag{6.6}$$

where N is the number of half-cycles, Γ is the gamma function and m_f is the fatigue strength exponent and

$$\chi = \sum_{k-1}^{N-1}(N-k)\left[\alpha_{m_f}\rho_{ss}^2(k) + \beta_{m_f}\rho^4 ss(k)\right] \tag{6.7}$$

where ρ_{ss} is the autocorrelation of the stochastic process for the stress half-cycles, α_{m_f} and β_{m_f} are coefficients depending on m_f obtained by curve-fitting techniques. The variance of the damage can then be obtained as

$$\sigma_D^2 = c_D^2 \bar{D}^2 \tag{6.8}$$

where $\bar{D}$ is the total expected damage. Low concludes that the proposed method is nearly exact up to around $m_f = 6$ and the method when applied to process that are less narrowband presents some minimal errors.

Garbatov and Soares [14] studied the effect of various factors related to fatigue damage assessment of a welded ship structural component. The considered factors were model of the ship, scatter diagram, heading and wave spectra. The fatigue damage was calculated using a spectral approach, considering the long-term stress range distribution as a series of short-term Rayleigh distributions for different sea states and headings.

They concluded that there are significant differences between all the pairs of fatigue damage means as function of the model of the ship, there are significant differences between the mean fatigue damage pairs of some of the heading directions, the mean fatigue damages as function of the scatter diagrams for North Atlantic and World Wide Trade are similar but for all the others testes scatter diagram there were significant differences and finally that for the three considered wave spectra there were also significant differences on the obtained fatigue damage.

7
Results

The expected damage on the critical point of the tower shown on Fig. 4.2 will be calculated. The working life of the equipment is 20 years. The main parameters of the platform and of the tower are shown on Tab. 7.1.

Table 7.1: Main parameters of the equipment

Diameter of the legs of the platform	D_c	27 m
Distance between the legs X dir.	L	70 m
Distance between the legs Y dir.	L	50 m
Draft of the platform	DR	15 m
Mass of the platform	M_P	15.000 t
Height of the tower	H	60 m
Height of the cross section	h	8 m
Width of the cross section	$b(x)$	7 m to 6 m
Thickness of the plates of the tower	t	24 mm to 15 mm
Hydrodynamic mass coefficient	a	760 t
Hydrodynamic damping coefficient	b	68 t/s
Weibull parameter for H_s	γ	0.84
Weibull parameter for H_s	m	1.6
Weibull parameter for H_s	β	1.6
S-N curve parameter	m_{f1}	3
S-N curve parameter	C_{f1}	$10^{12.592}$
S-N curve parameter	m_{f2}	5
S-N curve parameter	C_{f2}	$10^{16.320}$
Stress concentration factor	SCF	1

The Pierson-Moskowitz spectrum has been used to identify the frequency composition of the sea surface wave elevation. The spectrum is shown on Fig. 7.1.

For each simulation the phase angles for the different frequencies of sea surface elevation were randomly chosen between 0 and 2π rad. The probability density function for the phase angles was considered to be uniform.

On Fig. 7.2 one can see a snapshot of the sea surface elevation obtained using the PM spectrum. The sea surface elevation was calculated and a realization of the elevation at two of the cylinders of the platform is shown on Fig. 7.3.

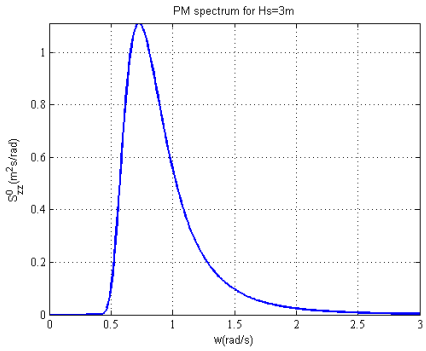

Figure 7.1: PM spectrum

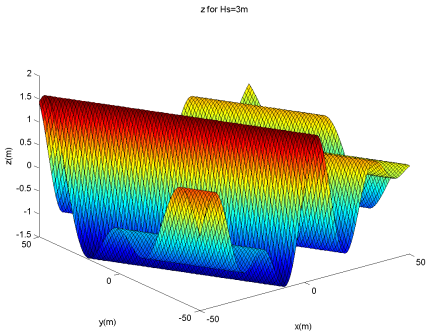

Figure 7.2: Sea surface elevation

A KL decomposition of the sea surface elevation was accomplished in order to reduce the computational cost of calculating the dynamic response of the platform. The simulation was carried out for 10s. After the simulation the KL basis has been obtained and the results have been approximated using only 6 modes. The construction of KL basis took 5% of the necessary time to construct the original model. On Fig. 7.4 one can see a comparison between the original result from simulation and the result obtained from reduced-order model for all the points on the field at a given instant. A good agreement between both results can be noted.

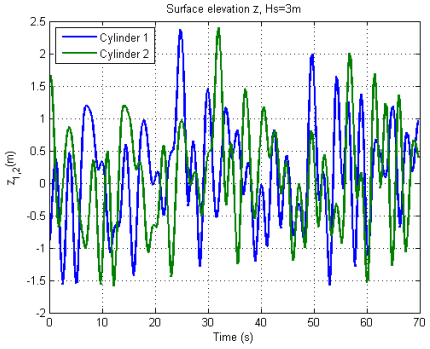

Figure 7.3: Sea surface elevation at cylinders

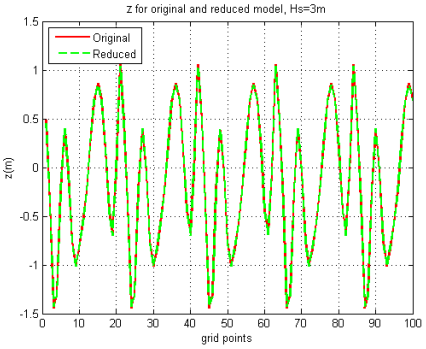

Figure 7.4: Original x reduced-order model

The Froude-Krilov forces on the bottom of the cylinders are the only external forces acting on the platform. A realization of theses forces is shown on Fig. 7.5. The incidence angle χ is randomly chosen between 0 and 2π rad. The probability density function for this incidence angle was considered to be uniform. This choice applies for moored platforms on locations where there are no prevailing wind directions.

The dynamics of the platform is given by Eq. (7.1). The restitution coefficient is given by Eq. (3.35). The remaining parameters are given on Tab. 7.1. A realizations of platform displacement is shown on Fig. 7.6.

$$\begin{bmatrix} M_P + 4a & 0 & 0 \\ 0 & I_{xx} + 2aL_y^2 & -I_{xy} \\ 0 & -I_{xy} & I_{xx} + 2aL_x^2 \end{bmatrix} \begin{Bmatrix} \ddot{z} \\ \ddot{\phi} \\ \ddot{\theta} \end{Bmatrix} + \begin{bmatrix} 4b & 0 & 0 \\ 0 & 2bL_y^2 & 0 \\ 0 & 0 & 2cL_x^2 \end{bmatrix} \begin{Bmatrix} \dot{z} \\ \dot{\phi} \\ \dot{\theta} \end{Bmatrix}$$
$$+ \begin{bmatrix} 4c & 0 & 0 \\ 0 & 2cL_y^2 & 0 \\ 0 & 0 & 2cL_x^2 \end{bmatrix} \begin{Bmatrix} z \\ \phi \\ \theta \end{Bmatrix} = \begin{Bmatrix} (F_1 + F_2 + F_3 + F_4) \\ (F_3 + F_4 - F_1 - F_2)\, L_y \\ (F_2 + F_4 - F_1 - F_3)\, L_x \end{Bmatrix} \quad (7.1)$$

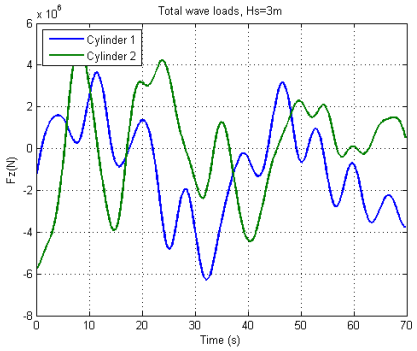

Figure 7.5: Total wave loads

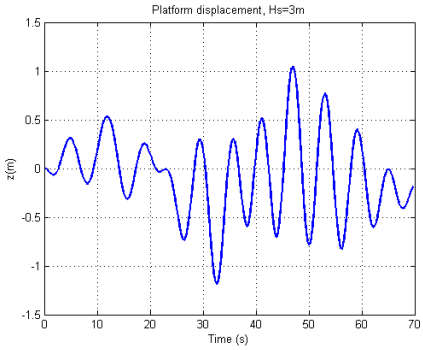

Figure 7.6: Platform displacement

The Weibull parameters for the significant wave height at the area where the structure will be installed are given on Tab. 7.1. The expected working years per each significant wave height are shown on Tab. 7.2.

Table 7.2: Significant wave height probability

H_S (m)	Prob.	Working years
1	0.0248	$t_1 = 0.496$
2	0.4252	$t_2 = 8.503$
3	0.3514	$t_3 = 7.028$
4	0.1474	$t_4 = 2.948$
5	0.0413	$t_5 = 0.827$
6	0.0084	$t_6 = 0.169$
7	0.0013	$t_7 = 0.026$
8	0.0002	$t_8 = 0.003$

The lifting load will be considered a concentrated mass at the free end of the beam/drilling tower. As the equipment is not always lifting the maximum load and there are limitations for the maximum load depending on the sea condition and it is necessary to estimate during design phase of the equipment the rate of use of the equipment for each expected sea condition. The maximum lifting load of the equipment is 800ton and this is the maximum value of the

concentrated mass, M_c. The rates of utilization of the equipment under each sea condition are given on Tab. 7.3.

Table 7.3: Rates of utilization of the equipment

Condition	-	1	2	3	4	5	6	7	8	9	10
h_S	m	1	1	1	1	1	2	2	2	2	2
Time	years	$\frac{t_1}{5}$	$\frac{t_1}{5}$	$\frac{t_1}{5}$	$\frac{t_1}{5}$	$\frac{t_1}{5}$	$\frac{t_2}{5}$	$\frac{t_2}{5}$	$\frac{t_2}{5}$	$\frac{t_2}{5}$	$\frac{t_2}{5}$
Conc. mass	ton	0	$\frac{M_c}{4}$	$\frac{M_c}{2}$	$\frac{3M_c}{4}$	M_c	0	$\frac{M_c}{4}$	$\frac{M_c}{2}$	$\frac{3M_c}{4}$	M_c
Condition	-	11	12	13	14	15	16	17	18	19	20
h_S	m	3	3	3	3	3	4	4	4	4	4
Time	years	$\frac{t_3}{5}$	$\frac{t_3}{5}$	$\frac{t_3}{5}$	$\frac{t_3}{5}$	$\frac{t_3}{5}$	$\frac{t_4}{5}$	$\frac{t_4}{5}$	$\frac{t_4}{5}$	$\frac{t_4}{5}$	$\frac{t_4}{5}$
Conc. mass	ton	0	$\frac{M_c}{4}$	$\frac{M_c}{2}$	$\frac{3M_c}{4}$	M_c	0	$\frac{M_c}{4}$	$\frac{M_c}{2}$	$\frac{3M_c}{4}$	M_c
Condition	-	21	22	23	24	25	26	27	28		
h_S	m	5	5	5	6	6	6	7	8		
Time	years	$\frac{t_5}{3}$	$\frac{t_5}{3}$	$\frac{t_5}{3}$	$\frac{t_6}{3}$	$\frac{t_6}{3}$	$\frac{t_6}{3}$	t_7	t_8		
Conc. mass	ton	0	$\frac{M_c}{4}$	$\frac{M_c}{2}$	0	$\frac{M_c}{4}$	$\frac{M_c}{2}$	0	0		

After the definition of the expected working conditions the dynamic simulations using a reduced order model for the finite element model was accomplished. A realization of the time history of the stress cycles at the critical point is shown on Fig. 7.7.

The steady-state part of the response is a stationary and ergodic process, therefore only one realization is needed, since a convergence check is accomplished. An histogram of the values of stress at a critical point of the structure obtained during the simulation is shown on Fig. 7.8.

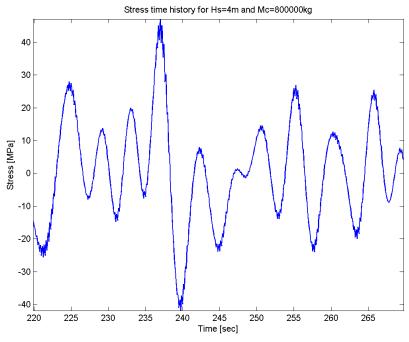

Figure 7.7: Stress time history at critical point

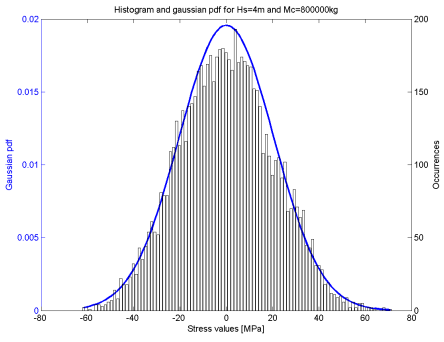

Figure 7.8: Histogram and Gaussian pdf

The rainflow procedure proposed by Nieslony [28] was used to determine the quantity of stress cycles per stress block. The obtained histogram and the Weibull pdf for the stress ranges are shown on Fig. 7.9.

The simulation period was 1000s and it was considered to be representative of a 3 hours sea state for the given significant height.

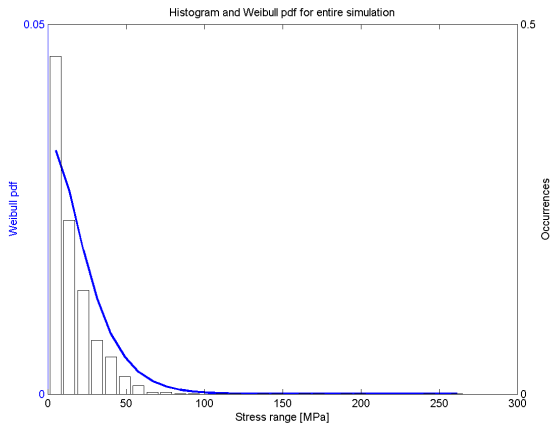

Figure 7.9: Histogram and Weibull pdf for entire simulation

The drilling tower is built from ten sections with different thickness welded to each other and welded to the deck of the platform. Each section in turn is built from four steel plates with same thickness, as shown on Fig. 4.2. Despite of the recommendation for doing a non destructive examination after the welding process, [6], there is always some level of misalignment between the plates and the welds can not be considered to have its nominal thickness all over its length. The thickness of the steel plates is not constant all over its area as well.

Such variations on the parameters of the structure must be considered during the evaluation of the fatigue resistance of the equipment otherwise the obtained value may be to conservative. The thicknesses of the welds between the sections of the tower will be considered a random variable ranging from 80% to 100% of the thickness of the plates. Due the uncertainty on the manufacturing process of the steel plates the thickness of the plates within the length of each finite element will be considered a random variable ranging from 100% to 105% of the nominal thickness of the plates. A correlation length of 0.01 between the thickness of the different welds and between the thickness of the plates within each finite element has been considered.

During the Monte Carlo simulation for the evaluation of the mean value and variance of the fatigue resistance it is necessary to simulate all the sea and loading conditions for each trial of the random parameters. Since the quantity of sea and loading conditions is significant it is necessary to reduce the computational effort as much as possible.

The Tab. 7.4 shows a few statistics for the results obtained after the Monte Carlo simulation.

Table 7.4: Influence of the uncertainty

Fatigue Damage				First Natural Frequency [Hz]			
Min.	Max	Mean	Std. Var.	Min.	Max	Mean	Std. Var.
0.57	1.04	0.71	0.15	2.99	3.01	3.00	0.004

8
Conclusions

In this work a computational model was developed to evaluate the structural integrity of a drilling tower welded to an offshore platform. The base of the tower is excited by the dynamics of the platform which in turn is excited by the ocean waves.

The Pierson-Moskowitz spectrum has been used to identify the frequency composition of the sea surface wave elevation. This spectrum can be used only after the wind has blown constantly for a certain period of time and the sea elevation surface becomes stationary. In this case the sea is referred to as *fully-developed*. In this work it was considered that during the entire working life the platform will be installed in an area whose sea surface elevation can be simulated using this spectrum. For ships or platforms that can work on different ocean areas and under different conditions alternative spectra may be necessary.

The geometry of legs of the platform has been simplified to four cylinders. In modern design of offshore platforms the legs can have rectangular cross section and be connected by floating pontoons. For a better simulation of the dynamics of the platform the interaction between sea water and these pontoons have to be evaluated. This is a difficult computational task and in this case the use of reduction-order models for the simulation of the sea surface elevation would bring great benefits. A reduced-order model for the sea surface elevation has been used and a good agreement between the results from the original and reduced-order model has been obtained.

The Froude-Krilov forces were the only considered external loads acting on the platform. In a more complex model additional loads as the drag forces can be considered.

The platform was considered a rigid body and the tower was excited at base due to the dynamic response of the platform. In case the flexibility of the platform was included on the system the bending of the deck of the platform is an additional source of deformation and consequently stresses to the welds at the base of the tower.

An approximation to the dynamic response of the drilling tower has been

obtained using a reduced-order finite element model. Since the external loads are presented as a base excitation it was necessary to include prescribed modes on the base of normal modes used to project the dynamics of the system. Up to the author's knowledge there are no publications about methods of obtaining such prescribed modes. The results obtained using the prescribed modes were compared with the ones obtained by the complete model and good agreement has been obtained. The method is time consuming, even for simplified models, which means that it is necessary to reduce the computational cost using reduced-order models as much as possible.

From results shown on Tab. 7.2 one can note that the main contribution for the fatigue damage is given by the significant wave heights of 3, 4 and 5m, therefore in case of a design change only these heights need to be simulated initially.

The choice of the period of simulation has a significant influence on the results, thus only the interval of the stress time history where the results are stable should be considered.

The lifting load was considered a concentrated mass at the free end of the beam/drilling tower. Such simplification can have significant influence on the obtained results. Jia [17] presented a method of calculating the fatigue damage on offshore jacket structures and concluded that the inertia effects of the structure, equipment mass in the structure and other non-structural installations have a significant contribution to fatigue damage. Elshafey et al [8] investigated the dynamic response of a scale model of an offshore jacket structure both theoretically and experimentally. They investigated the effects over dynamic response of changing the weights over the deck and noted that in some cases resonance may occur. They investigated the influence of the peak frequency of the wave spectra over the dynamic response as well. Therefore the influence of the simplifications on the construction of the model of the system should be carefully investigated.

At the realization of the time history of the stress cycles at the critical point shown on Fig. 7.7 one can note that there are several small range cycles along the time history. Such small range cycles are accounted for during the fatigue damage evaluation procedure but have no significant contribution for the damage.

It can be noted that the histogram shown on Fig. 7.8 can be approximated by a Gaussian probability density function with zero mean. It should be clear that this histogram is for the values of stress, peaks and valleys, and that stress range distribution, used to calculate the fatigue damage, is shown on histogram of Fig. 7.9 that was approximated to a Weibull probability density function.

In future works it can be investigated whether the Weibull distribution can be obtained from the Gaussian distribution.

It can be noted that the uncertainty on the on the thickness of the weld and on the thickness of the plates can cause some calculated fatigue damage to be above the acceptable level of 1 but has little influence on the dynamics of the structure. Therefore during Monte Carlo simulation different trials for the thickness of the weld and for the thickness of the plates can be use without calculating the dynamic response of the tower again. It will reduce the computational cost of the simulation.

In order to evaluate the fatigue resistance of a structural detail of a drilling tower installed on an offshore platform it was necessary first evaluate the sea surface elevation to be able to obtain the loads over the platform. Such loads have been used to obtain the dynamics of the platform and consequently the base excitation over the tower and its dynamic response. From the deformation of the tower the stress time history at the structural detail can be obtained and the fatigue resistance can be calculated. Despite of this being a long path to obtain the desired result the results have shown to be necessary to follow it.

The existing standards for fatigue resistance evaluation of offshore equipments present simplified analysis procedures based on long-term stress range distributions that depend on parameters that can not be determined a priori. Several different stress range distribution from other authors have been presented in this work and in all of them two or more parameters have to be determined. Some closed form solutions for obtaining these parameters have been presented but in some cases they have to be obtained using some source of curve fitting technique.

Some of the presented solutions are based on assumptions about the process being narrow-banded. When the designer is investigating some structure for the first time this kind of information is not available. When some kind of joint probability function for the parameters is necessary it has to be evaluated in some way.

Therefore the use of presented method is recommended when the designer has no previous information about the behavior of all the components of the system. Even initially using simplified models for the components such models can be replaced by more sophisticated ones at latter stages of the design process. The use of simplified models can provide valuable information about the behavior of the system.

After obtaining the histogram for the stress ranges the adjust to a curve is worthwhile. The histogram of stress ranges obtained for the studied detail

has shown to be similar to a Weibull distribution. Such approximation can be used within an optimization strategy to find a robust design, since the parameters of the distribution can be obtained without a complete simulation be accomplished. The Eqs. 5.20 and 5.20 are proposed as an alternative for calculating the fatigue damage when the stress range distribution follows a Weibull distribution.

Bibliography

[1] ANG, A. H. S.; CHEUNG, M. C.; SHUGAR, T. A. ; FERNIE, J. D. Reliability-based fatigue analysis and design of floating structures. **Marine Structuresv**, v.14, p. 25–36, 2001.

[2] BASILEVSKY, A. **Factor Analysis and Related Methods. Theory and Applications**. John Wiley & Sons, INC, 1994.

[3] BATOU, A.; SOIZE, C. Stochastic modeling and identification of an uncertain computational dynamical model with random fields properties and model uncertainties. **Archive of Applied Mechanics**, v.83, p. 831–848, 2013.

[4] BENAROYA, H.; HAN, S. M. **Probability Models in Engineering Science**, volume 1-2. CRC Press Taylor & Francis Group, Boca Raton, 2005.

[5] DNV. **DNV-RP-C203 - Fatigue Design of Offshore Steel Structures**. Det Norske Veritas, 2010.

[6] DNV. **DNV-RP-C206 - Fatigue Methodology of Offshore Ships**. Det Norske Veritas, 2010.

[7] DONG, W.; ET AL. Long-term fatigue analysis of multi-planar tubular joints for jacket-type offshore wind turbine in time domain. **Engineering Structures**, v.33, p. 2002–2014, 2011.

[8] ELSHAFEY, A.; ET AL. Dynamic response of offshore jacket structures under random loads. **Marine Structures**, v.22, p. 504–521, 2009.

[9] ETUBE, L. S. **Fatigue and Fracture Mechanics of Offshore Structures**. Professional Engineering Publishing Limited, 2001.

[10] FORRISTALL, G. Z. Maximum wave heights over an area and the air gap problem. **Proceedings of OMAE06, Hamburg, Germany**, 2006.

[11] FORRISTALL, G. Z. Wave crest heights and deck damage in hurricanes Ivan, Katrina and Rita. **Offshore Technology Conference, Houston, Texas**, 2007.

[12] FORRISTALL, G. Z. Maximum crest heights under a model tlp deck. **Proceedings of the ASME 2011 30th International Conference on Ocean, Offshore and Arctic Engineering, Rotterdam, The Netherlands**, 2011.

[13] FRICKE, W.; ET AL. Comparative fatigue strength assessment of a structural detail in a containership using various approaches of classification societies. **Marine Structures**, v.15, p. 1–13, 2002.

[14] GARBATOV, Y.; SOARES, C. G. Uncertainty assessment of fatigue damage of welded ship structural joints. **Engineering Structures**, v.44, p. 322–333, 2012.

[15] JAYNES, E. Information theory and statistical mechanics. **The Physical Review**, v.106(4), p. 1620–1630, 1957.

[16] JAYNES, E. Information theory and statistical mechanics ii. **The Physical Review**, v.108, p. 171–190, 1957.

[17] JIA, J. An efficient nonlinear dynamic approach for calculating wave induced fatigue damage of offshore structures and its industrial applications for lifetime extension. **Applied Ocean Research**, v.30, p. 189–198, 2008.

[18] JOURNÉE, J. M. J.; MASSIE, W. W. **Offshore Hydromechanics**. Delft University of Technology, 2001.

[19] KUKKANEN, T. **Spectral fatigue analysis for ship structures**. Helsinki, 1996. Licenciate's Thesis, Helsinki University of Technology. (in English).

[20] KUKKANEN, T. Fatigue design of offshore floating structures. **Proceedings of The Thirteenth International Offshore and Polar Engineering Conference**, p. 186–193, 2003.

[21] LANGLEY, R. S. Techniques for assessing the lifetime reliability of engineering structures subjected to stochastic loads. **Engineering Structures**, v.9, p. 95–103, 1987.

[22] LEIRA, B. J. Probabilistic assessment of weld fatigue damage for a nonlinear combination of correlated stress components. **Probabilistic Engineering Mechanics**, v.26, p. 492–500, 2011.

[23] LOÈVE, M. **Probability Theory, Graduate Texts in Mathematics, fourth edition**. Springer, USA, 1977.

[24] LOW, Y. M. A method for accurate estimation of the fatigue damage induced by bimodal processes. **Probabilistic Engineering Mechanics**, v.25, p. 75–85, 2010.

[25] LOW, Y. M. Variance of the fatigue damage due to a Gaussian narrowband process. **Structural Safety**, v.34, p. 381–389, 2012.

[26] LOW, Y. M.; CHEUNG, S. H. On the long-term fatigue assessment of mooring and riser systems. **Ocean Engineering**, v.53, p. 60–71, 2012.

[27] MCCORNICK, M. E. **Ocean Engineering Mechanics with Applications**. Cambridge University Press, 2010.

[28] NIESLONY, A. Determination of fragments of multiaxial service loading strongly influencing the fatigue of machine components. **Mechanical Systems and Signal Processing**, v.23, p. 2712–2721, 2009.

[29] PÉREZ, T.; BLANKE, M. **Simulation of Ship Motion in Seaway**. Australia: The University of Newcastle, 2002. 13p. Technical Report EE02037.

[30] RITTO, T. G.; BUEZAS, F. S. ; SAMPAIO, R. A new measure of efficiency for model reduction: Application to a vibroimpact system. **Journal of Sound and Vibration**, v.330, p. 1977–1984, 2011.

[31] SACRAMENTO, V.; SAMPAIO, R. ; RITTO, T. G. Fatigue damage of a drilling tower induced by ocean waves, accepted manuscript. **Journal of Brazilian Sciences and Mechanical Engineering**, v.In printing, p. In printing, 2013.

[32] SAMPAIO, R.; RITTO, T. G. **Short Course on Dynamics of Flexible Structures - Deterministic and Stochastic Analysis**. PUC-Rio, 2008.

[33] SARKAR, S.; GUPTA, S. ; RYCHLIK, I. Wiener chaos expansions for estimating rain-flow fatigue damage in randomly vibrating structures with uncertain parameters. **Probabilistic Engineering Mechanics**, v.26, p. 387–398, 2011.

[34] SCLAVOUNOS, P. D. Karhunen-loeve representation of stochastic ocean waves. **Proceedings of the Royal Society**, v.468, p. 2574–1594, 2012.

[35] SHANNON, C. E. A mathematical theory of communications. **Bell System Technical Journal**, v.27, p. 379–423,623–659, 1948.

[36] SUTHERLAND, H. J.; VEERS, P. S. Effects of cyclic stress distribution models on fatigue life predictions. **Wind Energy**, v.16, p. 83–90, 1995.

[37] TASDEMIR, A.; NOHUT, S. Fatigue analysis of ship structures with hinged deck design by finite element method. A case study: Fatigue analysis of the primary supporting members of 4900 PCTC. **Marine Structures**, v.25, p. 1–12, 2012.

[38] VELDKAMP, D. A probabilistic evaluation of wind turbine fatigue design rules. **Wind Energy**, v.11, p. 655–672, 2008.

[39] WANG, Y. Spectral fatigue analysis of a ship structural detail. A practical case study. **International Journal of Fatigue**, v.32, p. 310–317, 2010.

[40] WU, M.; HERMUNDSTAD, O. A. Time-domain simulation of wave-induced nonlinear motions and loads and its applications in ship design. **Marine Structures**, v.15, p. 561–597, 2002.